Journal of Information Hiding and Multimedia Signal Processing ©2024 ISSN 2073-4212
Ubiquitous International Volume **15**, Number **4**, December **2024**

Enhanced Brain Tumor Detection via Multiscale Frangi Gaussian Matrix and Efficient Convolutional Networks on MRI

Sheethal. M. S*

Research Scholar, Department of CSE,
Avinashilingam Institute for Home Science & Higher Education for Women,
[1] sheethalbasil@gmail.com

P. Amudha[2]

Professor, Department of CSE
Avinashilingam Institute for Home Science & Higher Education for Women
[2] amudha_cse@avinuty.ac.in

*Corresponding author: Sheethal. M. S

Received August 1, 2024, revised October 18, 2024, accepted October 22, 2024.

Abstract. *A brain tumor is an abnormal cell growth in or around the brain, which is benign or malignant. MRI scans are extensively used for their high resolution and superior contrast, enabling precise classification of brain tumors. However, accurate identification of brain tumors through MRI scans is crucial, hence a novel, Multiscale Frangi susceptibility Cat Randomized Gaussian Gray-level Matrix has been proposed to classify brain tumors using MRI. Which, MRI data extraction faces challenges due to partial volume effects, tissue misclassification, and dynamic venous blood flow, particularly in intertwined vessels and neural tissue. Thus, the Dynamic Multiscale Frangi susceptibility-weighted Contrast is introduced, and the multiscale Frangi filter enhances the vessel structures across different scales. Susceptibility-Weighted Imaging (SWI) and Dynamic Susceptibility Contrast (DSC) within a stacked CNN architecture integrating these techniques, for enhancing clinical interpretation accuracy and reliability. Furthermore, limited research on brain tumor classification using Venous Collateralization Patterns and Peritumoral Edema Characteristics is delayed by existing imaging markers, due to a lack of standardized protocols, and poor accuracy. So, Extreme Spatial Channel Cat Randomized Trees are presented with Spatial Channel-Wise Attention (SCA), CatBoost and Extremely Randomized Trees (ERT). Incorporating these methods into a stacked CNN to enhance the precision of brain tumor classification. Moreover, existing algorithms struggle to accurately measure tumor spatial distribution and complex morphological variations, limiting their ability to accurately measure lacunarity value and delay survival rate predictions. Therefore, the Gaussian Gray-level size length matrix was offered through the utilization of the Gray-Level Run Length Matrix (GLRLM), Gray-Level Size Zone Matrix (GLSZM), and Gaussian Kernel by incorporating in the Stacked CNN layer, it enhances prediction accuracy by accurately capturing the spatial distribution of gaps or clusters within tumors, improving tumor morphology understanding and patient care.*
Keywords: Brain Tumor Classification, Intertwined Vessels, Neural Tissue, Complex Vascular Patterns, Vessel Structure Enhancement

1. **Introduction.** Brain tumors, abnormal growths of cells within the brain, manifest with a myriad of symptoms ranging from headaches and seizures to cognitive impairment

and personality changes. Early diagnosis is crucial in mitigating potential complications and improving treatment outcomes. Magnetic Resonance Imaging (MRI) plays a pivotal role in the detection and classification of brain tumors due to its unparalleled ability to provide detailed images of the brain's anatomy and pathology. By utilizing powerful magnetic fields and radio waves, MRI produces high-resolution images that aid in identifying the location, size, and characteristics of tumors within the brain. Moreover, advanced MRI techniques such as diffusion-weighted imaging and perfusion imaging offer insights into tumor aggressiveness and vascularity, facilitating precise diagnosis and treatment planning. With its non-invasive nature and superior imaging capabilities, MRI significantly contributes to the early detection and accurate classification of brain tumors, thereby guiding clinicians in delivering timely and tailored interventions to patients for optimal outcomes and improved quality of life [1-4].

In classifying benign and malignant brain tumors such as Gangliоglioma, Oligodendroglioma, Schwannoma, Ependymoma, Glioblastoma, and Medulloblastoma using extracted cerebral venous system features from MRI, various feature extraction and segmentation methods are employed. These include region-based methods like thresholding and clustering, which segment brain structures based on intensity or statistical properties, while edge-based methods detect boundaries using gradient information. Hybrid approaches, such as active contours and machine learning algorithms like convolutional neural networks (CNNs), combine both region and edge information for improved accuracy. Challenges arise due to the intricate nature of cerebral venous structures, which is challenging to separate from surrounding tissues, especially in the presence of noise, intensity in homogeneities, and anatomical variability in MRI images. Furthermore, the distinction between benign and malignant tumors based solely on venous features extracted from MRI is complex, as these tumors may exhibit similar vascular patterns. Additionally, the computational complexity and time-consuming nature of some segmentation methods pose practical challenges in clinical settings, emphasizing the need for robust algorithms capable of accurately extracting cerebral venous system features for effective tumor classification and diagnosis [5-8].

After extracting the features, classification methods are employed for classifying the brain tumors using MRI, including Venous Collateralization Patterns and Peritumoral Edema, ranging from conventional SVMs, decision trees, and random forests to deep learning CNNs. SVMs and decision trees handle high-dimensional data but may struggle with complex feature relationships, while random forests mitigate overfitting but lack interpretability. Deep learning, notably CNNs, excels at feature extraction but demands extensive annotated data and computational resources. Challenges include accurately delineating tumor borders, discerning edema from healthy tissue, and variability in imaging protocols affecting results. Integrating multi-modal data and addressing class imbalance are additional hurdles. Concerns about the interpretability of deep learning models continue to hinder their clinical acceptance. Mitigation strategies involve data augmentation, transfer learning, and ensembling for improved generalization in brain tumor classification [9-12].

Moreover, after classifying the tumor then predicts the survival rate of patients. These include traditional machine learning techniques such as logistic regression, support vector machines (SVM), random forests, and artificial neural networks (ANNs). Additionally, more advanced approaches like convolutional neural networks (CNNs) have been increasingly explored due to their ability to automatically extract features from MRI images. Challenges in these methods arise from the complexity and heterogeneity of brain tumors, which make accurate prediction difficult. Limited sample sizes and data imbalance further compound these challenges, leading to issues with overfitting and generalization.

Moreover, preprocessing MRI data to extract relevant features while minimizing noise and artifacts adds another layer of complexity. Interpretability of results and the integration of clinical data with imaging data also pose significant challenges in accurately predicting survival rates. Additionally, ensuring the robustness and reproducibility of predictive models across different patient cohorts and imaging protocols remains a key concern. Overall, while these methods show promise, addressing these challenges is crucial to improving the accuracy and reliability of survival rate predictions for brain tumor patients using MRI data [13-15]. Even though there are many developments in the detection and classification of brain tumors using MRI, there are still many improvements needed to enhance the classification accuracy by solving issues in the extraction of features from MRI and classifying the tumor using those features and other limitations in the present research. Major contributions of this paper are given below

- To improve the delineation of complex vessel networks, particularly in regions where vessels are intertwined with neural tissue, a novel Dynamic Multiscale Frangi susceptibility-weighted Contrast has been proposed, which effectively utilizes the strengths of each method to simplify cerebral venous system extraction from MRI, enhancing clinical interpretation accuracy and reliability.
- To classify brain tumor using Venous Collateralization Patterns and Peritumoral Edema Characteristics, a novel Extreme Spatial Channel Cat Randomized Trees is introduced, this enhances brain tumor classification accuracy by addressing collateralization and optimizing the utilization of comprehensive imaging markers.
- To accurately measure tumor spatial distribution and complex morphological variations, a novel Gaussian Gray-level size length matrix is presented, which enhances prediction accuracy by accurately capturing the spatial distribution of gaps or clusters within tumors, improving understanding of tumor morphology and enhancing patient care.

The paper's content is structured as follows: Section 2 covers the literature survey, discussing existing contributions relevant to classifying brain tumor with MRI scans. Section 3 outlines the proposed methodology and its functioning. Section 4 delves into the evaluation, performance, and comparative analysis of the proposed model. Lastly, Section 5 provides the conclusion for the paper.

2. **Literature Survey.** Javeria et al [16] suggested a fully automated heterogeneous segmentation system utilizing support vector machines (FAHS-SVM) for deep learning-based brain tumor segmentation. The current work suggests adding a new, totally automatic approach based on anatomical, morphological, and relaxometry features to separate the entire cerebral venous system into MRI imaging. A high degree of homogeneity between the architecture and surrounding brain tissue characterizes the segmenting function. An ELM is a kind of learning algorithm that has one or more hidden node layers. The probabilistic neural network classification method has been used to train and assess the tumor detection accuracy in brain MRI images. However, the drawback of the proposed approach was its reliance on predetermined features, potentially limiting adaptability to diverse datasets and reducing overall segmentation accuracy due to feature selection biases.

Yakub et al [17] suggested a Faster R-CNN deep learning system that used the Region Proposal Network (RPN) to mark the location of the tumor's appearance. There are three main types of brain cancers in the chosen MR imaging dataset: glioma, meningioma, and pituitary. The region proposal network and the classifier network in the suggested approach both use the VGG-16 architecture as their foundation layer. The algorithm's detection and classification findings show that it detected gliomas with an average precision of 75.18%, meningiomas with an average precision of 89.45%, and pituitary tumors

with an average precision of 68.18%. However, the proposed method suffers from reduced performance in detecting pituitary tumors compared to other types, indicating potential limitations in generalization across different tumor classes.

Milica et al [18] developed a novel CNN architecture for the categorization of three different forms of brain tumors. The created network was evaluated on T1-weighted contrast-enhanced magnetic resonance imaging, and it was less complex than previously developed pre-trained networks. Four methods were used to assess the network's performance: two databases and two combinations of two 10-fold cross-validation techniques. The network's capacity to generalize was evaluated using subject-wise cross-validation, one of the ten-fold approaches, and its improvement was evaluated using an enhanced picture database. However, the proposed method faced challenges in scalability and generalization to new datasets due to its specific design tailored to T1-weighted contrast-enhanced MRI, potentially limiting its applicability in broader clinical contexts.

Cheng et al [19] aimed to determine whether the meningioma's PTBE volume and its diffusion and perfusion characteristics correlate. Retrospectively analyzed 70 consecutive individuals with meningiomas who had preoperative DTI and DSC-PWI (mean age, 58.9 ± 13.7 years; 37 women). The tumor's PTBE volume, tumor volume, mean T2 signal, ADC, FA, and CBV were all measured. T2 signal intensity, volume, ADC, FA, and CBV of tumors were evaluated between meningiomas with and without PTBE, as well as patient age and sex. T2 signal intensity, volume, ADC, FA, and CBV of tumors were analyzed in meningiomas with PTBE, along with correlations of PTBE volume with patient age and sex. To find the variables related to PTBE volume, multivariable linear regression analysis was done. However, the drawback lies in its retrospective design, which introduced biases and limitations in data collection and interpretation, affecting the reliability and generalizability of the correlation findings between meningioma characteristics and peritumoral edema volume.

Mobarakol et al [20] developed an attention-based convolutional neural network (CNN) to extract brain tumor information from MRIs. Additionally, use a variety of machine learning techniques to forecast the survival rate. Then, conduct segmentation by integrating channel and spatial attention with the decoder network using a 3D UNet architecture. Utilizing the geometry, position, and shape of the segmented tumor, extract some novel radiomic signals and combine them with clinical data to forecast the length of survival for each patient. To demonstrate the impact of each attribute on overall survival (OS) prediction, also conduct in-depth studies. However, the proposed approach encounters challenges in clinical adoption due to the complexity of integrating radiomic features with clinical data, potentially hindering interpretability and usability for healthcare practitioners. Lee et al [21] determined lacunarity and fractal dimension values for anomalies on gadolinium-enhanced T1-weighted magnetic resonance imaging (T1Gd MRI), T2-weighted (T2), and fluid-attenuated inversion recovery (FLAIR) MRIs that were caused by glioblastoma. Attempt to establish a relationship between the survival of GBM patients and these morphological parameters determined from pretreatment MRI in the patient cohort (n=402). Lacunarity and fractal dimension were computed on all MRI slices for necrotic regions (n = 390), abnormalities on T1Gd MRI (n = 402), and enhanced abnormalities on T2/FLAIR MRI (n = 257). Also, investigated how these parameters related to anomaly volume and age at diagnosis. For all three imaging subtypes, statistically significant associations with the final result; the most robust association was observed between the overall survival and the kind of T2/FLAIR abnormalities. However, the proposed method faces challenges in directly translating lacunarity and fractal dimension values into actionable clinical insights or treatment strategies, highlighting potential limitations in bridging the gap between radiological findings and patient outcomes.

Kibriya et al. [22] introduced a novel fully automated method for brain tumor identification and classification that combined hand-engineered and deep features to improve accuracy. The approach addressed the limitations of relying solely on deep learning algorithms, which typically require extensive labeled data. By incorporating a supervised approach, the method enhanced the classification process, surpassing existing methods in speed and accuracy for brain cancer detection. This framework provided a more efficient and precise diagnostic tool for medical professionals. By leveraging an ensemble of deep and hand-crafted features, the system enhanced discriminative capabilities in brain tumor detection. However, the focus was primarily on classification rather than segmentation, a critical step in the comprehensive analysis of medical images for diagnosis and treatment planning.

Sarkar et al [23] suggested using an AlexNet CNN to separate MRI datasets into training and test data, as well as for feature extraction, which enhanced classification accuracy. They employed BayesNet, SMO, NB, and RF classifiers to classify brain tumors as no-tumor, glioma, meningioma, and pituitary tumors, achieving high accuracy rates. The limitations of conventional machine learning techniques were addressed by automatically extracting important features using deep learning, leading to improved classification performance. The combination of AlexNet CNN feature extractor and prominent machine learning classifiers contributed to the field of medical image analysis. However, there was no exploration of the generalizability of the proposed model to different datasets or imaging modalities, limiting the broader applicability of the approach.

Archana et al [24] proposed a novel method, Bagging Ensemble with K-Nearest Neighbor (BKNN), to enhance the accuracy and quality rate of brain tumor identification using MRI images. This addresses the importance of accurate brain tumor detection using MRI imaging techniques and highlights the significance of early tumor detection for improved treatment options and patient survival rates. It emphasizes the use of U-Net architecture for image segmentation and a bagging-based k-NN prediction algorithm for classification, aiming to improve accuracy and parameter distribution in the layers. However, the segmentation outcomes heavily rely on the dispersion of training and testing models and features used, which affect the process of classification accuracy.

Ghafourian et al. [25] introduced a novel approach to diagnose brain tumors by integrating data mining and machine learning techniques, enhancing the efficiency of brain tumor detection in MR images. It utilizes the Social Spider Optimization (SSO) algorithm for MRI image segmentation, leading to more precise identification of tumor regions and extracts distinctive features using the SVD technique, which not only removes redundant information but also speeds up processing at the classification stage. By combining Naive Bayes, Support Vector Machine, and K-nearest neighbor algorithms, the model achieves high accuracy, sensitivity, and specificity in diagnosing brain tumors, surpassing previous efforts. However, the longer training time potentially impact the real-time applicability of the model in clinical settings.

From the above studies, it is clear that [16] decreasing segmentation accuracy overall and restricting adaptation to different datasets, [17] restrictions on generalization between various tumor classes, in [18] difficulties with scaling and generalizing to new datasets as a result of its unique architecture for T1-weighted contrast-enhanced magnetic resonance imaging, in [19] influencing the findings of the link between the volume of peritumoral edema and the characteristics of meningiomas, in [20] intricacy of combining radiomic features with clinical data presents adoption issues in the clinical setting, in [21] difficult to directly convert lacunarity and fractal dimension values into useful clinical insights or treatment plans, in [22] it focuses on the classification aspect of brain tumors using the

ensemble of features but does not delve into the segmentation of tumors, in [23] generalizability of the proposed model, limiting the broader applicability, in [24] segmentation outcomes heavily rely on the dispersion of training and testing models and features used, which can affect the process of classification accuracy, in [25] longer training time potentially impact the real-time applicability of the model. Hence, there is a need for a novel method to eliminate these drawbacks and increase the accuracy of the classification of brain tumors.

3. **Enhancing the Classification Accuracy of Brain Tumors using MRI.** Brain tumors are abnormal masses of cells that grow within the brain, potentially disrupting its functions and causing various neurological symptoms. Existing works utilize MRI scans for precise classification of brain tumors, which able to be benign or malignant, characterized by abnormal cell growth. However, the accurate classification of brain tumor using MRI scans are critical. Hence a novel, "Multiscale Frangi susceptibility Cat Randomized Gaussian Gray-level Matrix" has been proposed, to address the limitations from the existing studies and improve the classification accuracy of brain tumors using MRI. In which the cerebral venous system is crucial for tumor diagnosis and characterization. But, extracting it in MRI presents challenges due to partial volume effects and tissue misclassification. This is especially difficult in regions where vessels intertwine with arteries or neural tissue. The dynamic nature of venous blood flow also complicates signal interpretation, with slow or stagnant flow leading to signal loss and fast-flowing blood enhancing signal intensity.

To address this issue, a novel approach called Dynamic Multiscale Frangi susceptibility-weighted Contrast is introduced to enhance vessel structures across different scales by applying a multiscale Frangi filter. This model incorporates Susceptibility-Weighted Imaging (SWI) an advanced MRI technique that uses the magnetic properties (susceptibility) of different tissues to create high-contrast images of the brain, enhancing visualization of venous blood and vessel delineation and Dynamic Susceptibility Contrast (DSC) a functional MRI technique that evaluates cerebral blood flow and volume by tracking the passage of a contrast agent through the brain's vasculature, enabling the distinction between slow and fast blood flow. By integrating these techniques within a stacked Convolutional Neural Network (CNN) architecture, leverages the complementary strengths of each method. The CNN architecture allows for the efficient processing of MRI images, extracting relevant features, and making accurate classifications, thereby improving accuracy and reliability in clinical interpretation.

Additionally, MRI extracts from the cerebral venous system provide accurate classification of brain tumors like Ganglioglioma, Oligodendroglioma, Schwannoma, Ependymoma, Glioblastoma, and Medulloblastoma. Though, limited research focusing on classifying brain tumors using Venous Collateralization Patterns and Peritumoral Edema Characteristics, which are the features extracted from the cerebral venous system. Variations in vascular anatomy and drainage, along with factors like tumor size, location, and histological subtype, lead inconsistencies in collateralization patterns and peritumoral edema classification. However, existing classification methods struggle to adapt features like tumor size and shape to complex vascular patterns and edema characteristics due to traditional imaging markers and lack of standardized protocols for feature extraction and integration, leading to poor classification accuracy and complicating the integration of venous collateralization patterns and peritumoral edema characteristics. Thus, a novel Extreme Spatial Channel Cat Randomized Trees is presented, to address the challenges of existing methods and significantly improving classification accuracy. This model integrates Spatial Channel-Wise Attention (SCA) an advanced mechanism used in neural

networks, particularly in Convolutional Neural Networks (CNNs), to focus on informative input data, reducing irrelevant data and noise, enhancing feature representation and accurately capturing subtle differences between brain tumor types.

Similarly, by incorporating CatBoost a machine learning algorithm to handle categorical data efficiently and Extremely Randomized Trees (ERT), an ensemble learning method that builds multiple decision trees, where CatBoost is known for its handling of categorical features and robustness against overfitting, while ERT improves classification by averaging multiple, unpruned decision trees. By incorporating these techniques within a stacked Convolutional Neural Network (CNN) allows the model incorporates features related to the cerebral venous system and edema for accurate tumor classification, addressing standardized protocol issues and adapting to individual tumor characteristics. Furthermore, the classification of tumors focuses on patient survival rates, focusing on lacunarity values. However, extracting these values is complex due to the heterogeneous nature of the tumor.

Existing algorithms struggle to accurately measure the spatial distribution of gaps or clusters within tumors due to their reliance on predefined features and thresholds, which do not adequately represent the complex morphological variations in heterogeneous tumors, thereby delaying precise survival rate predictions based on lacunarity values. So, a novel Gaussian Gray-level size length matrix is introduced, to capture complex spatial and morphological variations that are critical for accurate predictions, it combines the principles of the Gray-Level Run Length Matrix (GLRLM) a statistical tool used to quantify texture in an image, to captures the length of consecutive gray level runs along specific directions, aids in identifying patterns and structures within images, aiding in the identification of different tissue types or abnormalities, and Gray-Level Size Zone Matrix (GLSZM), provides information on the size of homogeneous zones in an image, to quantifies the size of homogeneous zones in an image, providing insights into tumor structure and complexity by measuring clusters of pixels that share identical gray levels, and Gaussian kernels is a smoothing operator that emphasizes spatial relationships within the image by applying a Gaussian function to the pixel values, which enhances the visibility of spatial relationships by reducing noise and highlighting significant structures, making it easier to identify patterns and variations in the image.

After the features extracted from GLRLM and GLSZM, along with the smoothed image data from the Gaussian kernel, are fed into a Stacked (CNN) model which learn complex and non-linear relationships between the extracted features and survival outcomes. Consequently, the proposed method enhances prediction accuracy by accurately capturing tumor morphology's complex spatial distribution of gaps or clusters, thereby improving patient care.

Figure 1 depicts a complex process for classifying brain tumors using MRI scans, starting with input images processed through stages: extraction of the cerebral venous system, feature extraction focusing on Venous Collateralization Patterns and Peritumoral Edema Characteristics, classification using Extreme Spatial Channel Cat Randomized Trees within a stacked CNN architecture, and achieving high classification accuracy for various tumor types like Glioblastoma, Oligodendroglioma, Schwannoma, Ependymoma, and Medulloblastoma. The method integrates advanced imaging techniques and machine learning algorithms to improve accuracy, addressing challenges in medical imaging analysis and potentially improving patient outcomes. Additionally, the inclusion of the Gaussian Gray-level size length matrix enhances prediction accuracy by capturing complex spatial and morphological variations critical for accurate predictions, ultimately enhancing patient care.

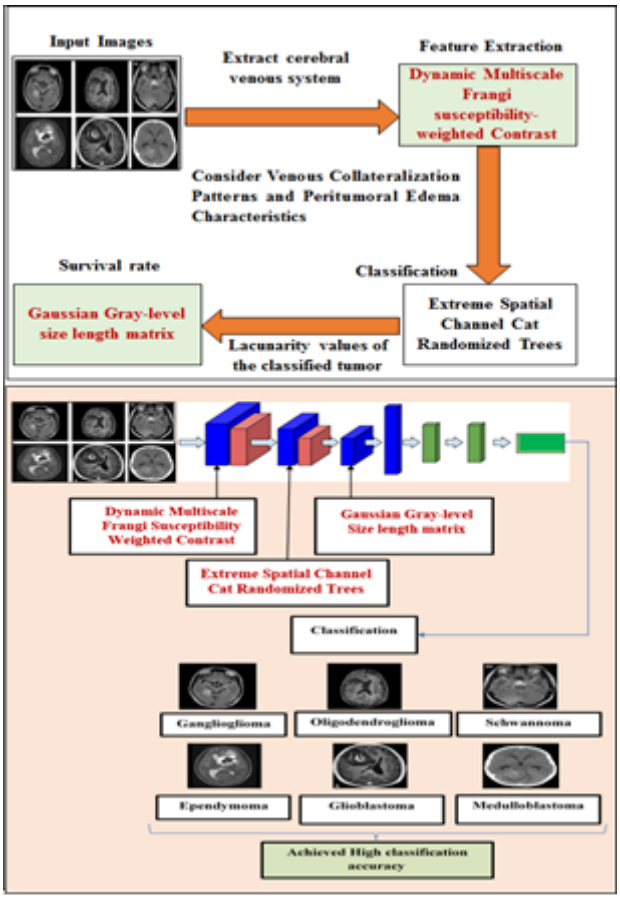

FIGURE 1. Block Diagram of Multiscale Frangi susceptibility Cat Randomized Gaussian Gray-level Matrix

3.1. **Improved Venous Vessel Visualization and Differentiation.** To tackle the complexities involved in extracting the cerebral venous system from MRI scans, the Dynamic Multiscale Frangi susceptibility-weighted contrast (DMFSWC) technique is introduced to enhance the visualization and differentiation of venous vessels from surrounding tissues, ultimately improving the classification accuracy of brain tumors. This technique integrates several methods to achieve its objectives. Initially, the Multiscale Frangi Filter enhances vessel structures across different scales, minimizing partial volume effects and aiding in the differentiation of intertwined vessels and neural tissue. Then, Susceptibility-Weighted Imaging (SWI) leverages susceptibility differences in tissues, particularly in venous blood, to improve their visualization. SWI enhances the delineation of venous vessels from surrounding structures, aiding in their identification and differentiation. Finally, Dynamic Susceptibility Contrast (DSC) provides dynamic information about blood flow, allowing discrimination between slow or stagnant flow and fast-flowing blood. By integrating these methods within a stacked CNN architecture, the technique capitalizes on the complementary strengths of each, addressing the intricacies associated with cerebral venous system extraction from MRI scans. The following subsections explained above statements.

Stacked CNN, this method uses MRI data, undergoes convolution, multiple filters, susceptibility weighted imaging, dynamic susceptibility contrast, within a stacked CNN architecture to process features, resulting in cerebral venous structures.

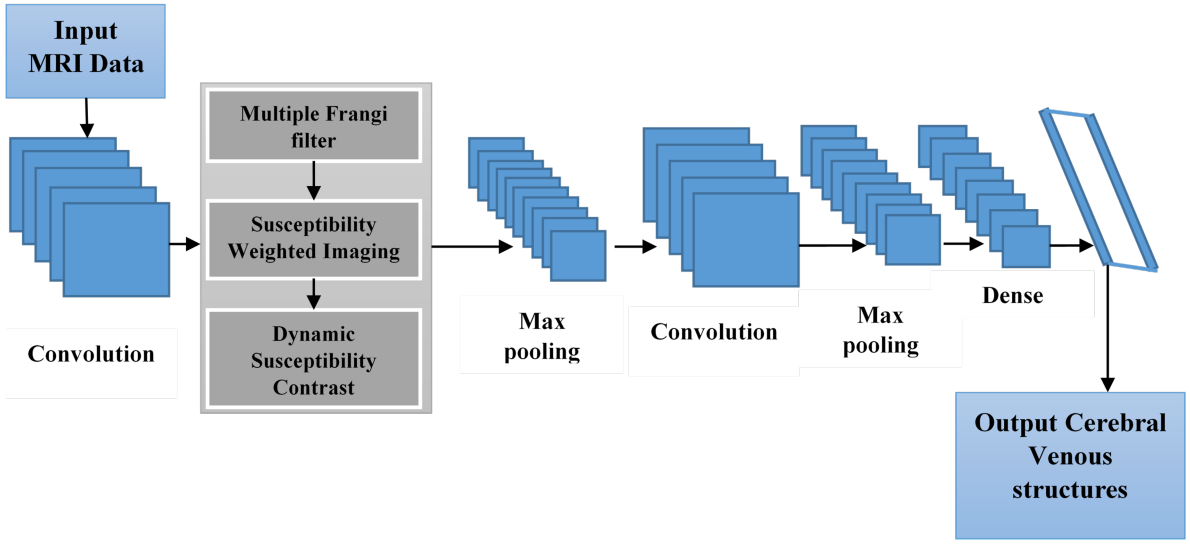

FIGURE 2. Dynamic Multiscale Frangi susceptibility-weighted contrast within Stacked CNN

3.1.1. *Multiscale Frangi Filter.* To enhance and extract vessel-like structures from images, an image processing technique named Multiscale Frangi Filter is used. It is a variant of the Frangi filter that operates across multiple scales, enabling it to capture vessels of different sizes within an image. Multiscale Frangi filtering is a powerful technique used to enhance linear structures such as blood vessels in medical images. This filtering is based on analyzing the local curvature of the image intensity using the Hessian matrix. The first step involves computing the Hessian matrix of the image. The Hessian matrix is a square matrix of second-order partial derivatives that describes the local curvature of a function. For an image I, the Hessian matrix H at each pixel is given in equation (1) [26]:

$$H = \begin{bmatrix} I_{xx} & I_{xy} \\ I_{yx} & I_{yy} \end{bmatrix} \tag{1}$$

In the above equation, the second partial derivatives of image I are specified as I_{yx}, I_{xy}, I_{xx}, and I_{yy}, in which I_{xx} is in x direction, I_{yy} is in y direction and I_{xy} and I_{yx} are in xy direction. The two eigenvalues corresponding to the Hessian matrix, are λ_1 and λ_2, and it reveals information about the curvature of the image intensity.

Eigenvalue λ_1: Represents the curvature in the direction where the change in intensity is minimal.

Eigenvalue λ_2: Represents the curvature in the direction where the change in intensity is maximal.

For a vessel-like structure, $|\lambda_1| \ll |\lambda_2|$ indicates a small gradient in one direction and a larger gradient in the perpendicular direction. It suggests that one direction has little change, while the perpendicular direction has a steep change.

To quantify the vessel-likeness of a structure, two key ratios are used, Boldness Ratio R_b given in equation (2):

$$R_b = \left| \frac{\lambda_1}{\lambda_2} \right| \tag{2}$$

Where, R_b measures the relative magnitudes of the eigenvalues λ_1 and λ_2. For vessel-like structures, R_b should be small because $|\lambda_1|$ is much smaller than $|\lambda_2|$, and Second-Order

Structure Measure S given in equation (3):

$$S = \sqrt{\lambda_1^2 + \lambda_2^2} \tag{3}$$

Where, S quantifies the overall magnitude of the eigenvalues, reflecting the intensity of the local structure. A higher value of S indicates stronger features in the image.

Then measure Vesselness V_σ at a pixel to quantify by combining the two feature operators to produce a response of highlighted vessel-like structures, given in the equation (4):

$$V_\sigma = \begin{cases} 0, & \lambda_2 > 0 \\ \exp\left(-\frac{R_b^2}{2\beta^2}\right)\left(1 - \exp\left(-\frac{S^2}{2c^2}\right)\right), & \lambda_2 \leq 0 \end{cases} \tag{4}$$

When $\lambda_2 > 0$: The response is zero, indicating no vessel-like structure.

When $\lambda_2 \leq 0$: The response is calculated using: $\exp\left(-\frac{R_b^2}{2\beta^2}\right)$ suppresses blob-like structures by being sensitive to R_b. A small R_b means a stronger response. Then $1-\exp\left(-\frac{S^2}{2c^2}\right)$ emphasizes areas with strong structure S, leading to higher responses in vessel-like regions. The parameters β and c are assigned for tuning the sensitivity of features concerning Frangi filter and need to be tuned based on the specific application and characteristics of the image.

For reducing high-frequency noise Gaussian filtering is used, which interferes with the Hessian matrix calculations. The Gaussian filter for an image I at a point (x, y) is given in equation (5):

$$G_\delta(x, y) = \frac{1}{2\pi\delta} \exp\left(-\frac{x^2 + y^2}{2\delta^2}\right) \tag{5}$$

The δ, which is the variable parameter, specifies the convolutional scale corresponding to Gaussian filter. Larger values of δ lead to increased smoothing, effectively reducing noise and making it easier to identify and enhance linear structures within the image. This process helps to clarify the image by diminishing high-frequency noise, thereby facilitating the detection of features like blood vessels.

Vessel structures appear at various scales within an image. To effectively capture vessels of different sizes, the Frangi filter is applied at multiple scales, which is given in equation (6):

$$V_0 = \max_\delta(V(\delta)) \tag{6}$$

By adjusting the parameter δ, the filter is capable of detecting structures of varying sizes, from small to large vessels. The final vesselness value V_0 for each pixel is determined as the maximum response across all scales, ensuring that the most significant vessel-like structure at that specific location is emphasized.

After applying the Frangi filter and aggregating the responses across multiple scales, the resulting image undergoes normalization to a standardized range, typically between 0 and 255. This harmonizes the pixel values, ensuring that vessel structures stand out distinctly against the background. This adjustment is essential for facilitating clear visualization and detailed analysis of the vascular network. The Frangi filter utilizes the Hessian matrix to assess local curvature in an image, focusing on enhancing linear structures like blood vessels based on their specific curvature properties. Through eigenvalue analysis and feature operators, it identifies these structures by integrating information across multiple scales, effectively highlighting them across varying sizes and orientations. Before normalization, Gaussian filtering is applied to reduce noise, ensuring clearer detection of vessel-like features. This preprocessing step enhances the accuracy of identifying

blood vessels, making the subsequent analysis more reliable and conducive to detailed medical imaging applications.

3.1.2. *Susceptibility-Weighted Imaging (SWI).* After applying the Multiple Frangi filter in the Dynamic Multiscale Frangi Susceptibility-Weighted Contrast approach, the focus shifts to enhancing the visualization of venous structures by leveraging magnetic susceptibility differences between tissues. This technique, known as Susceptibility-Weighted Imaging (SWI), capitalizes on the distinct magnetic properties of veins compared to surrounding brain tissue such as gray and white matter.

SWI operates by utilizing both magnitude and phase information obtained from MRI scans, which are highly sensitive to magnetic susceptibility variations. It employs high-resolution gradient-echo imaging coupled with phase information acquisition to effectively highlight veins and other structures with unique magnetic characteristics, thereby maximizing sensitivity to susceptibility effects. The enhanced image contrast provided by SWI is crucial for accurately delineating brain vasculature and detecting abnormalities such as tumors and vascular malformations. SWI complements Frangi filtering, which identifies vessel-like structures based on geometric features, by offering additional high-contrast information based on magnetic properties.

The integration of SWI into the Dynamic Multiscale Frangi Susceptibility-Weighted Contrast approach further enhances diagnostic accuracy by combining SWI with Frangi filtering and other imaging modalities. This comprehensive method enables precise visualization of venous involvement around tumors and facilitates the assessment of potential vascular complications. Moreover, SWI contributes valuable insights into the relationships between brain structure and function, supporting the monitoring of disease progression over time and aiding in clinical decision-making.

3.1.3. *Dynamic Susceptibility Contrast (DSC).* Dynamic imaging is a magnetic resonance imaging (MRI) technique used primarily to assess cerebral blood flow dynamics. It provides valuable information about the perfusion characteristics of tissues, including the brain, by measuring changes in the MRI signal intensity over time following the injection of a contrast agent (typically a gadolinium-based contrast agent).

DSC imaging relies on the principle that contrast agents alter the relaxation times (T1 and T2*) of tissues they perfuse. When a contrast agent is administered, it induces a temporary reduction in MRI signal intensity owing to its paramagnetic characteristics, influencing the local magnetic field and leading to signal attenuation. DSC provides real-time information on blood flow by measuring alterations in MRI signal intensity caused by the transit of the contrast agent through the vasculature. The temporal evolution of signal intensity changes reflects the flow of contrast through arteries, capillaries, and veins, enabling evaluation of perfusion parameters such as cerebral blood volume (CBV), cerebral blood flow (CBF), and mean transit time (MTT).

- Cerebral Blood Volume (CBV): DSC estimates CBV, which is a measure of the total volume of blood in a given region of brain tissue. This is essential for assessing tumor vascularity, as tumors often exhibit increased CBV compared to normal brain tissue.
- Cerebral Blood Flow (CBF): It provides insights into the rate of blood flow through brain tissue, helping to assess perfusion patterns. Changes in CBF indicate regions of hypoperfusion or hyperperfusion, which may be indicative of pathology such as ischemia or tumor growth.
- Mean Transit Time (MTT): MTT represents the average time taken for blood to pass through a specified region of brain tissue. It reveals the abnormalities in vascular function and is useful in evaluating treatment responses in conditions like stroke or brain tumors.

These parameters aid in diagnosing brain tumors, assessing treatment responses, and monitoring vascular dynamics critical for neurological conditions. DSC aids in assessing tumor vascularity by comparing tumor tissue to normal brain tissue, with highly vascularized tumors showing higher CBV and CBF values and it also supports treatment planning and monitoring, assessing response to treatments like chemotherapy and radiation therapy, and detecting changes in perfusion parameters post-treatment.

Dynamic Susceptibility Contrast offering dynamic information on cerebral blood flow that is crucial for diagnosing, characterizing, and monitoring brain tumors and other neurological disorders. Its ability to quantify perfusion parameters such as CBV, CBF, and MTT ultimately improving diagnostic accuracy and treatment planning. DSC complements the multiscale Frangi filter and susceptibility-weighted imaging (SWI) components of the technique by providing additional information on blood flow dynamics. It helps in distinguishing between slow-flowing and fast-flowing blood, which is critical for accurate interpretation of venous structures and their relationship to brain tumors.

3.1.4. *Extracting relevant features, for Accurate Classifications.* The ESCCRT (Extreme Spatial Channel Cat Randomized Trees) framework integrates advanced techniques within a stacked CNN architecture to enhance the classification of brain tumors from MRI scans. Traditional methods typically focus on basic imaging markers such as tumor size and shape, which may overlook crucial details like venous collateralization patterns and peritumoral edema characteristics. ESCCRT leverages deep learning capabilities to extract and process complex features directly from MRI data.

By incorporating spatial channel-wise attention and randomized trees, ESCCRT effectively capture intricate information inherent in the cerebral venous system and other advanced imaging modalities like SWI and DSC. This approach ensures that the model robustly differentiate between different types of brain tumors based on comprehensive and detailed features. Ultimately, ESCCRT aims to improve classification accuracy by providing a more sophisticated and reliable framework compared to existing methods, thereby advancing the field of neuroimaging diagnostics and enhancing patient care outcomes.

Figure 3 depicts the flowchart for Dynamic Multiscale Frangi Susceptibility-Weighted Contrast (DMFSWC). The process begins with data preprocessing, which includes initialization and input of data. A Multiscale Frangi Filter is applied to enhance vessel structures across different scales, mitigating partial volume effects and aiding in the differentiation of intertwined vessels and neural tissue. Gaussian smoothing is applied to the images, and images are normalized to enhance visualization of vessel structures. Susceptibility-Weighted Imaging (SWI) is applied to improve the visibility of venous blood by exploiting its susceptibility differences. Dynamic Susceptibility Contrast (DSC) is applied to provide dynamic information about blood flow, enabling the discrimination between slow or stagnant flow and fast-flowing blood, thereby enhancing vessel identification. The enhanced images are integrated into a stacked CNN architecture, fed into the CNN model, trained on the enhanced images, and extracted complex features. The output features from the trained model are obtained, and the process ends. This simplified flowchart provides a visual representation of the proposed method, addressing challenges in extracting cerebral venous systems and classifying brain tumors more accurately by enhancing feature representation and capturing complex vascular patterns.

3.2. **Improving Classification Accuracy.** The Extreme Spatial Channel Cat Randomized Trees (ESCCRT) technique is introduced in the proposed method for brain tumor classification to overcome limitations in existing brain tumor classification methods, which often struggle with integrating complex vascular patterns and edema characteristics from MRI scans. By leveraging advanced ensemble learning techniques like CatBoost and

Algorithm 1 Dynamic Multiscale Frangi Susceptibility-Weighted Contrast (DMFSWC)

Input: MRI scans of the brain, Gadolinium-based contrast agent (for DSC)
Output: Enhanced visualization of cerebral venous structures

Start:
Step 1: Preprocessing
Input the MRI scans.
Normalize the images to a standard intensity range (0-255).
Apply Gaussian smoothing to reduce high-frequency noise.
Step 2: Multiscale Frangi Filter
Compute the Hessian Matrix H for the image.
Compute the eigenvalues λ_1 and λ_2 of the Hessian matrix.
Compute the Blobness Ratio R_b and Second-Order Structure Measure S.
Calculate the vesselness measure V_σ for each pixel.
Apply the filter across multiple scales δ and determine the maximum response.
Normalize the resulting image to enhance vessel structures.
Step 3: Susceptibility-Weighted Imaging (SWI)
Acquire high-resolution gradient-echo MRI images.
Utilize both magnitude and phase information to emphasize susceptibility differences.
Phase information is especially useful for highlighting veins due to their magnetic susceptibility.
Combine magnitude and phase data to enhance venous structure visualization.
Step 4: Dynamic Susceptibility Contrast (DSC)
Inject the gadolinium-based contrast agent.
Perform dynamic MRI scanning to track the contrast agent's passage through the brain's vasculature.
Measure changes in MRI signal intensity over time.
Calculate perfusion parameters:
- Cerebral Blood Volume (CBV)
- Cerebral Blood Flow (CBF)
- Mean Transit Time (MTT)

Use DSC data to differentiate between slow-flowing and fast-flowing blood.
Step 5: Integration into Stacked CNN Architecture
Feed the enhanced images from Frangi filter, SWI, and DSC into a stacked CNN.
Implement Spatial Channel-Wise Attention (SCA) to focus on relevant features.
Utilize CatBoost and Extremely Randomized Trees (ERT) for robust classification.
Train the CNN model to learn intricate spatial patterns and morphological variations from the processed MRI data.
Step 6: Feature Extraction and Classification
Extract complex features such as venous collateralization patterns and peritumoral edema characteristics.
Output classified visualization of cerebral venous structures.
End

Extremely Randomized Tree (ERT) alongside Spatial Channel-Wise Attention (SCA), to enhance the models ability to accurately classify tumors based on intricate features extracted from imaging data.

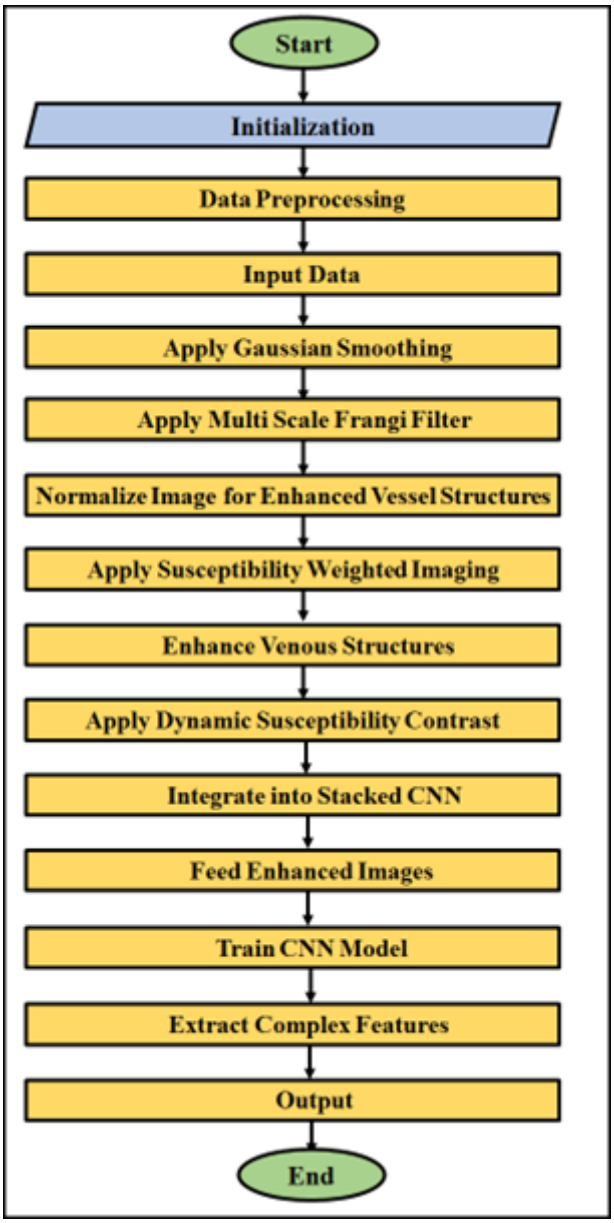

FIGURE 3. Flowchart for Dynamic Multiscale Frangi Susceptibility-Weighted Contrast

Figure 4 illustrates Extreme Spatial Channel Cat Randomized Trees with Stacked CNN involves input MRI scans of cerebral vessels, convolution, SCA block, CatBoost and Extremely Randomized Trees, with in the Stacked CNN's convolution and max pooling layers, and a final Dense layer for brain tumor classification, integrating venous features for improved classification.

3.2.1. *Capture Complex Vascular Patterns and Edema Characteristics.* Spatial Channel-Wise Attention (SCA) plays a crucial role in enhancing feature representation by selectively focusing on informative channels within the data. In the context of brain tumor classification from MRI scans, SCA can effectively capture complex vascular patterns and edema characteristics extracted from the cerebral venous system. By integrating SCA into the classification framework, the model can prioritize channels that contain critical information related to venous collateralization patterns and peritumoral edema.

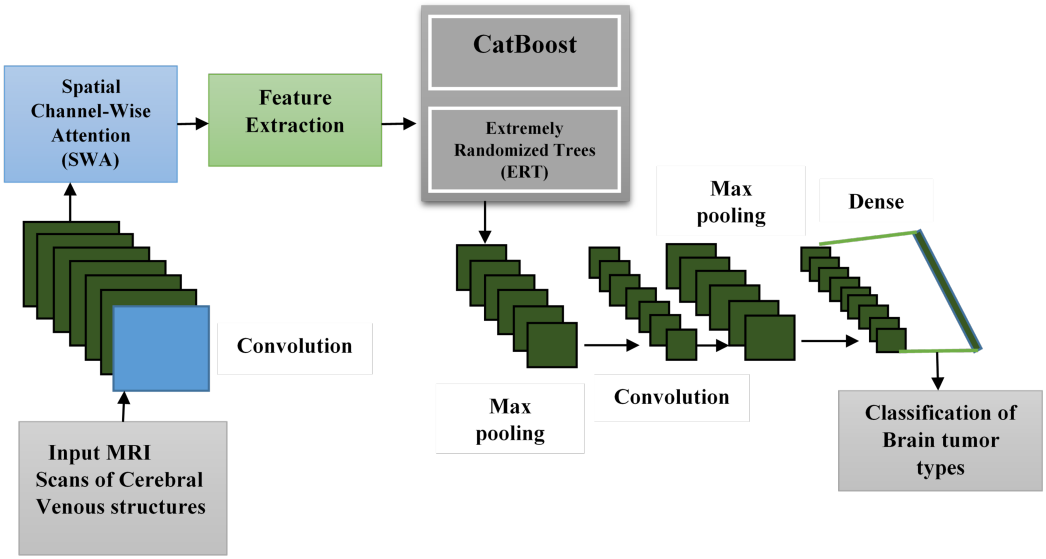

FIGURE 4. Extreme Spatial Channel Cat Randomized Trees with Stacked CNN

SCA combines the feature map F_l with the saliency map S_l to identify regions of interest in the image. Then calculate the compatibility score in the ith region, c_i, between F_l and S_l. It is computed using the dot product of their respective vectors u, a learnable parameter, and normalized using softmax as given in equation (7) [27]:

$$c_i = (u, f_l) + s_i \tag{7}$$

Where, f_l are the feature maps from F_l, and s_i are elements from S_l. Softmax operation normalizes the compatibility score c_i into attention coefficients, which highlight emotionally relevant regions α_i given in equation (8).

$$\alpha_i = \frac{\exp(c_i)}{\sum_j \exp(c_j)} \tag{8}$$

Where, c_j is the compatibility score in the jth region. Each feature map f_l^i is weighted by its corresponding attention coefficient α_i given in equation (9).

$$U = \sum \alpha_i \cdot f_l^i \tag{9}$$

Where U is the aggregated output obtained by weighting each feature map, and f_l^i represents the ith feature map in the lth layer. Global average pooling aggregates spatial information X across U dimensions into a channel descriptor z_c given in equation (10).

$$z_c = \frac{1}{X \times X} \sum_{i=1}^{X} \sum_{j=1}^{X} u_c(i, j) \tag{10}$$

Where u_c specifies the channel c of feature map at position (i, j). Channel-wise statistics z_c are passed through excitation functions to emphasize informative channels given in equation (11).

$$s = \sigma(W_2 \cdot \mathrm{ReLU}(W_1 z_c)) \tag{11}$$

Where, W_1 and W_2 are learned weights, $ReLU$ is a non-linear activation function and σ is the sigmoid activation function. Channel u_c is weighted by activations s_c to produce the final output e_{fc} given in equation (12).

$$e_{fc} = F_{\text{scale}}(u_c, s_c) = u_c s_c \tag{12}$$

F_{scale} represents the collection of all e_{fc}, emphasizing channel-wise importance in capturing complex vascular patterns and edema characteristics crucial for accurate brain tumor classification.

3.2.2. *Improving the Adaptability of the Model.* CatBoost and Extremely Randomized Trees (ERT) are powerful ensemble learning algorithms used for supervised classification tasks. CatBoost, an advanced gradient boosting decision tree method, addresses prediction shift and statistical challenges by iteratively improving predictions while handling categorical features robustly through ordered boosting. It enhances model accuracy by minimizing loss functions iteratively. Also, ERT, an extension of random forest methodology, excels in accuracy by leveraging multiple decision trees that vote collectively on predictions. It accommodates large datasets without feature deletion, evaluates variable importance comprehensively, and ensures efficiency in handling multi-dimensional input characteristics.

CatBoost is based on gradient boosting decision trees and addresses prediction shift by iteratively refining predictions through ordered boosting. The training process aims to minimize the expected loss function $L(F)$, where $F(t)$ represents the predicted output for input t. The iterative update formula for CatBoost is given in equation (13) [28]:

$$F_t = F_{t-1} + \alpha h_t \tag{13}$$

Where, F_t is the prediction at iteration t, F_{t-1} is the prediction at iteration $t-1$, α is the learning rate and h_t is the base predictor function at iteration t. CatBoost enhances accuracy by sequentially improving the predictions based on the residuals.

ERT extends the random forest methodology by using multiple decision trees to collectively determine predictions. It excels in accuracy by averaging the predictions from numerous decision trees. The training process involves building multiple trees on random subsets of the data and features. The predicted output $F(t)$ at particular instance t is determined by the voting mechanism across these trees given in equation (14) [29]:

$$F(t) = \frac{1}{N} \sum_{i=1}^{N} f_i(t) \tag{14}$$

Where f_i is the function of pixel-wise vector at i^{th} decision tree, N is the total number of decision trees in the ensemble model used to calculate the average prediction. By incorporating, CatBoost and ERT iteratively improve predictions (CatBoost through boosting iterations and ERT through averaging multiple trees) to achieve high accuracy in classification tasks, handling complex datasets with varying features and ensuring robust performance in machine learning applications.

3.2.3. *Accurately Differentiating Brain Tumor Types.* A stacked CNN architecture enhancing the analysis of MRI data, particularly for brain tumor classification. By stacking multiple convolutional layers, this architecture excels in extracting hierarchical features from complex MRI images. It integrates advanced techniques such as Susceptibility-Weighted Imaging (SWI) and Dynamic Susceptibility Contrast (DSC), which enhance the visualization and analysis of the cerebral venous system. SWI highlights venous blood by exploiting susceptibility differences, while DSC provides dynamic blood flow information.

This deep learning framework enables the CNN to learn intricate spatial relationships within the MRI data, crucial for accurately differentiating brain tumor types based on features like venous collateralization patterns and peritumoral edema characteristics. The stacked architecture's ability to process these diverse features ensures robust classification performance, surpassing existing methods reliant on simpler imaging markers.

Algorithm 2 Extreme Spatial Channel Cat Randomized Trees (ESCCRT)

Input: MRI scans of the brain with detailed venous structures and tumor characteristics.
Output: Accurate classification of brain tumor types.

Start:
Step 1: Initialization
Initialize parameters and data structures.
Step 2: Feature Extraction using SCA
Compute feature maps F_l from the input MRI using convolutional layers.
Generate a saliency map S_l to highlight informative regions.
Compute the compatibility scores c_i between f_l and S_l using the dot product.
Normalize c_i using softmax to obtain attention coefficients α_i.
Weight each feature map f_l by its attention coefficient α_i.
Aggregate spatial information across U dimensions using global average pooling to form channel descriptors.
Pass channel-wise statistic z_c through excitation functions to emphasize informative channels.
Weight channels u_c by activations s_c to produce the final output.
Step 3: Integration of CatBoost and ERT
Implement CatBoost and Extremely Randomized Trees (ERT) ensemble learning techniques.
Step 4: Model Training and Evaluation
Train the ESCCRT model using the combined output e_f from SCA and predictions from CatBoost and ERT.
Assess the model's performance using a validation set.
Step 5: Classification of Brain Tumor Types
Use the trained ESCCRT model to categorize types of brain tumors using extracted features such as venous collateralization patterns and peritumoral edema characteristics.
Step 6: Output
Output the classified brain tumor types along with confidence scores.
End

Figure 5 depicts the flowchart for Extreme Spatial Channel Cat Randomized Trees (ESCCRT). The process begins with initialization, which involves setting up data and model parameters. Spatial Channel-Wise Attention (SCA) is used to extract features from MRI data, enhancing feature representation. CatBoost and Extremely Randomized Trees (ERT) algorithms are integrated into the model, leveraging ensemble learning to handle variations in vascular anatomy and drainage across individuals. The model is trained on enhanced images and evaluated for performance, producing output features likely related to tumor classification results. This simplified flowchart provides a visual representation of the method, addressing challenges in extracting cerebral venous systems

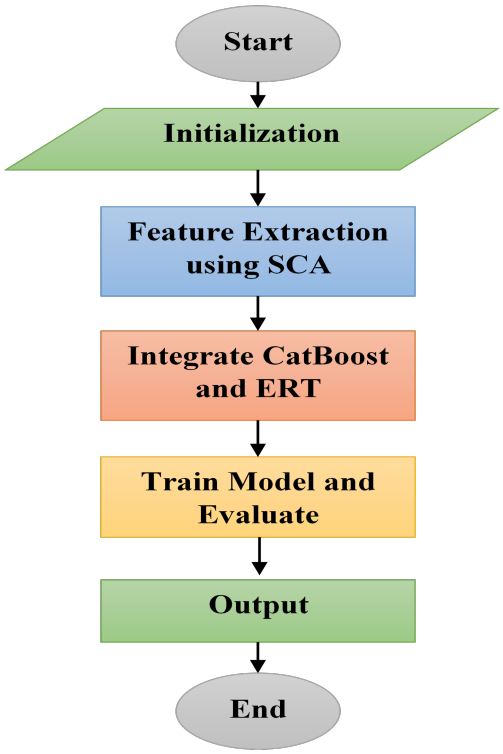

FIGURE 5. flowchart for Extreme Spatial Channel Cat Randomized Trees (ESCCRT)

and classifying brain tumors more accurately by enhancing feature representation and capturing complex vascular patterns.

3.3. **Analyzing Survival Rates from Extracted MRI Scans.** The Gaussian Gray-level Size Length Matrix (GGSLM) technique has been introduced to specifically tackle the complexities associated with analyzing survival rates based on lacunarity values extracted from brain tumor MRI scans. Brain tumors exhibit a heterogeneous nature, characterized by diverse spatial patterns and distributions of tumor components such as necrotic areas, cysts, and solid masses. Existing approaches struggle to accurately capture these variations, as they rely on predefined features that do not adequately represent the intricate spatial relationships within tumors. By incorporating Gray-Level Run Length Matrix (GLRLM), Gray-Level Size Zone Matrix (GLSZM), and Gaussian Kernel to improve the accuracy of survival rate predictions.

3.3.1. *Capturing Texture Information from MRI Images.* The GLRLM technique is introduced to effectively capture and quantify texture information within brain tumor MRI scans. Its primary purpose is to analyze the length of consecutive pixels exhibiting the same gray-level intensity across different directions, typically measured at 0°, 45°, 90°, and 135° angles. This approach enables the characterization of linear structures present in tumor components, such as necrotic areas, solid masses, and cysts. GLRLM operates by constructing matrices that count the occurrences of consecutive pixel runs for each gray-level intensity and direction, which extracts statistical measures from GLRLM matrices, including Short Run Emphasis (SRE), Long Run Emphasis (LRE), Gray-Level Non-Uniformity (GLN), Run Length Non-Uniformity (RLN), Run Percentage (RP), and Run Entropy (RE). By computing these run lengths, the technique provides detailed insights into the spatial distribution and arrangement of textures within the MRI images.

This information is crucial for understanding the internal morphology of brain tumors, which exhibit heterogeneous patterns and complexities that existing imaging markers overlook, and enhances the ability to distinguish between different tumor types based on their textural characteristics.

By integrating GLRLM into analysis within stacked CNN architectures, researchers and clinicians derive meaningful features that improve the accuracy of tumor classification and survival rate predictions. Thus, GLRLM contributes significantly to advancing the clinical interpretation of MRI data and enhancing decision-making in the management of brain tumors.

3.3.2. *Evaluating Size Variations of Homogeneous Zones.* The GLSZM technique is utilized to quantify and analyze size variations of homogeneous zones within brain tumor MRI scans. Its primary purpose is to assess the spatial distribution and size of homogeneous areas, providing valuable insights into the internal structure of tumors. GLSZM achieves this by calculating several metrics that describe the characteristics of these homogeneous zones. These metrics include measures of zone size variability and intensity variation across different regions of the image. By systematically analyzing these parameters, GLSZM helps in identifying and delineating distinct regions within the tumor, such as areas of uniform intensity or texture, and complements other image processing techniques by offering detailed information about the distribution of homogeneous zones. This information is critical for understanding the heterogeneous nature of tumors, where different regions exhibit varying sizes and intensities of homogeneous areas.

Integrating GLSZM into analytical frameworks, such as alongside Gray-Level Run Length Matrix (GLRLM) and other texture analysis methods within stacked CNN architectures, enhances the overall capability to characterize tumor morphology accurately. This comprehensive approach enables features that improve the classification of brain tumors based on their internal structure. Ultimately, it contributes to advancing the clinical interpretation of MRI data and supports more informed decision-making in the diagnosis and treatment planning for patients with brain tumors.

3.3.3. *Enhancing the Features of Spatial Distribution.* The Gaussian Kernel is employed to enhance the spatial relationships and reduce noise within the data extracted from techniques like GLRLM and GLSZM in the brain tumor analysis from MRI scans. Its primary purpose is to emphasize the spatial distribution of features, thereby ensuring that subtle variations in the arrangement of tumor components are accurately captured.

This technique works by convolving the image data with a Gaussian function, which effectively smooths out abrupt changes or noise in the spatial domain. By applying the Gaussian Kernel, the spatial representation of features derived from GLRLM and GLSZM is enhanced, leading to a more refined understanding of the spatial characteristics of brain tumors. This smoothing process is crucial as it helps to highlight meaningful spatial relationships while suppressing irrelevant variations or noise that may obscure important structural details within the MRI images. By integrating the Gaussian Kernel into the feature extraction process supports the accurate measurement of spatial patterns and morphological variations. It ensures that the extracted features are robust against minor inconsistencies in the image data, thereby improving the reliability of quantitative assessments of tumor characteristics.

By incorporating the Gaussian Kernel within a stacked CNN architecture alongside other advanced image processing techniques, such as GLRLM and GLSZM, the overall framework becomes more adept at capturing and interpreting the spatial complexities of brain tumors. This approach facilitates better characterization of tumor morphology

from MRI scans, aiding in more precise diagnosis, treatment planning, and monitoring of patients with brain tumors.

Algorithm 3 Gaussian Gray-level Size Length Matrix (GGSLM)

Input:
MRI scans of brain tumors
Output:
Texture information capturing spatial distributions and variations
Improved accuracy in survival rate predictions

Start:
Step 1: Preprocessing
Normalize MRI scans to a standard intensity range.
Apply Gaussian smoothing to reduce noise and enhance texture details.
Step 2: Gray-Level Run Length Matrix (GLRLM)
Compute GLRLM for each MRI scan to capture texture information.
Define directions (0°, 45°, 90°, 135°) for pixel run length calculations.
Construct matrices counting occurrences of consecutive pixel runs for each gray-level intensity and direction.
Step 3: Texture Feature Extraction
Extract statistical measures from GLRLM matrices.
Step 4: Gray-Level Size Zone Matrix (GLSZM)
Compute GLSZM to analyze size variations of homogeneous zones.
Calculate metrics to describe homogeneous zone sizes and intensity variations across different image regions.
Step 5: Integration with Gaussian Kernel
Convolve GLRLM and GLSZM data with a Gaussian Kernel to enhance spatial relationships and reduce noise.
Adjust kernel parameters (e.g., standard deviation) to optimize feature extraction.
Step 6: Feature Enhancement
Combine enhanced GLRLM and GLSZM features to capture comprehensive spatial distributions and morphological variations of brain tumors.
Step 7: Analysis and Interpretation
Utilize the enriched feature set for survival rate prediction analysis.
Evaluate the impact of spatial texture features on prediction and treatment planning.
End

Figure 6 outlines the Flowchart of Gaussian Gray-level Size Length Matrix. It begins with normalization, which involves setting up data and model parameters. The Gray-Level Run Length Matrix (GLRLM) is constructed and computed, capturing texture information within the MRI data. Texture features are extracted from this information. The Gray-Level Size Zone Matrix (GLSZM) is computed, quantifying size variations within the MRI data. The Gaussian Kernel is integrated into the model, emphasizing spatial relationships within the MRI data. Feature enhancement is done to improve representation. The enhanced features are analyzed and interpreted to make predictions about brain tumor classification and survival rate. The process ends with the process. This simplified

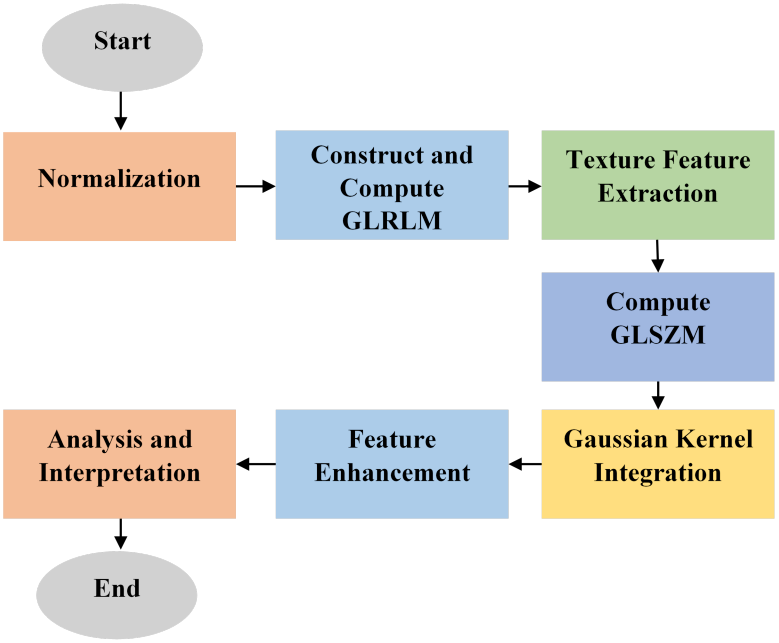

FIGURE 6. Flowchart of Gaussian Gray-level Size Length Matrix (GGSLM)

flowchart provides a visual representation of the proposed method, aiming to address challenges in extracting cerebral venous systems and classifying brain tumors more accurately. It is a useful tool for understanding the complex medical image processing technique.

Overall, the Dynamic Multiscale Frangi Susceptibility-Weighted Contrast approach is a new framework designed to improve brain tumor imaging and venous system visualization from MRI scans. It combines advanced imaging modalities and deep learning techniques to enhance visualization, classification, perfusion dynamics, and texture and spatial analysis. The method uses the Multiscale Frangi Filter and SWI to improve the clarity and contrast of cerebral venous structures, enabling accurate delineation of vasculature around tumors and detecting vascular anomalies. The ESCCRT framework within a stacked CNN architecture improves the classification of brain tumors, extracting intricate features related to vascular patterns and tumor characteristics from MRI data. DSC imaging provides dynamic information on cerebral blood flow, essential for assessing tumor vascularity and monitoring treatment responses. The GGSLM technique captures textural variations and spatial distributions within tumors, supporting survival rate predictions considering the heterogeneous nature of brain tumors. This approach represents a significant advancement in neuroimaging diagnostics, enhancing clinical decision-making and patient outcomes in neurology and oncology.

4. **Results and Discussion.**

This section presents the results achieved by the proposed model, showing significant improvements in brain tumor classification accuracy. Validation of the prediction accuracy was conducted by comparing it with other existing approaches.

4.1. **Tool & System Specification.**

- **Software:** Python
- **OS:** Windows 10 (64-bit)
- **Processor:** Intel i5
- **RAM:** 8GB RAM

4.2. **Dataset Description.** The datasets for the BraTS challenge have been updated since BraTS'18, now featuring more routinely acquired 3T multimodal MRI scans. Validation data will be released on July 15, allowing participants to generate preliminary results and include them in their submitted papers. Test data will be distributed via email between August 7 and September 7, with top-ranked teams invited to prepare slides for a brief oral presentation. This year's BraTS challenge includes training, validation, and testing datasets comprising pre-operative multimodal MRI scans of glioblastoma and lower grade glioma, accompanied by pathologically confirmed diagnoses and overall survival data. This dataset was taken from:
`https://www.kaggle.com/datasets/aryashah2k/brain-tumor-segmentation-brats-2019`
`https://www.kaggle.com/datasets/awsaf49/brats20-dataset-training-validation`

4.3. **Simulation Outputs of Suggested Model.** This section consists of the simulated results of the suggested model.

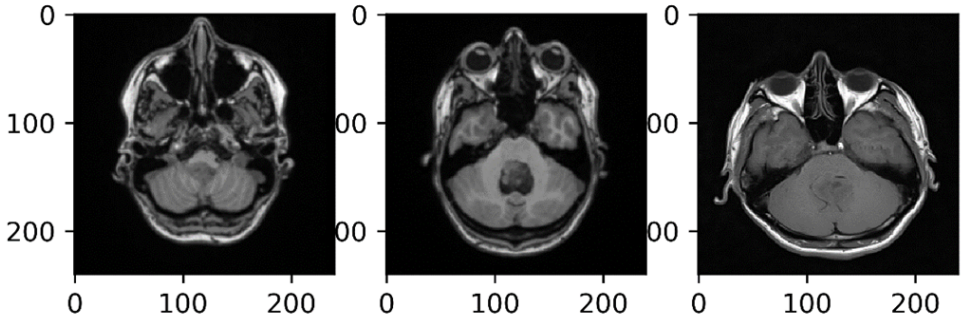

(A) Test Input Images

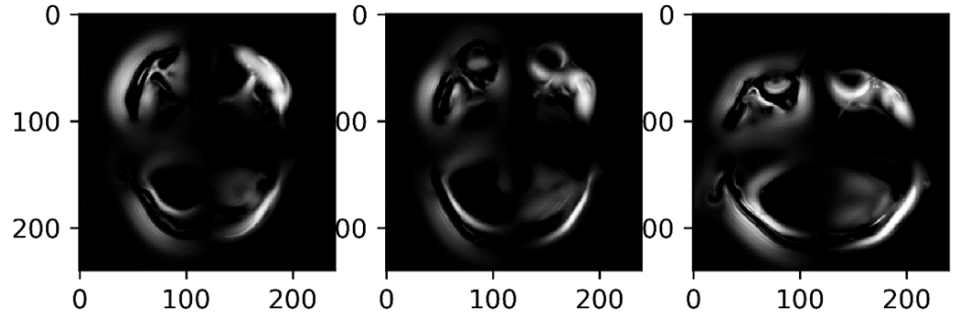

(B) Frangi Filter Response

FIGURE 7. Simulated Output Brain Classification using Frangi Filter

Figure 7 (a, b) represents the input images and Frangi filter response of three MRI brain scans, revealing the overall brain structure, abnormal tissue characteristics, and specific brain structures. These scans are crucial for medical diagnosis, treatment planning, and monitoring neurological conditions. The Frangi filter enhances the detection of tubular structures like blood vessels or airways by emphasizing their edges and suppressing other features.

This technique is useful in tasks like medical imaging analysis, where detecting vessels or tubular structures is crucial. The Frangi filter's response is demonstrated through grayscale plots, with darker areas indicating lower values and brighter areas indicating higher values. This variation in brightness demonstrates how the filter responds to different features within an image, making it valuable in brain tumor detection.

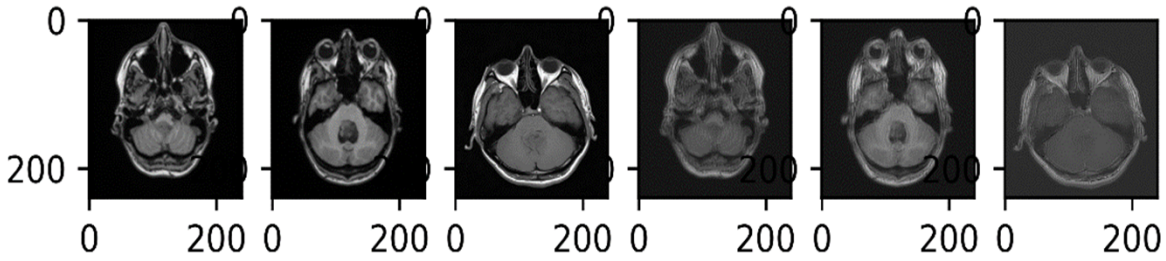

FIGURE 8. Tumor Detection (Input and CNN response images)

Figure 8 presents the axial MRI brain scans for tumor detection. The first scan, corresponding to a lower level of the brain, provides an overview of brain structures like the cerebral cortex, ventricles, and basal ganglia. The second scan, slightly higher, reveals more detailed features like the thalamus, hippocampus, and white matter tracts. The third scan, representing a central level, shows structures like the corpus callosum and lateral ventricles, and reveals pathological changes like tumors or vascular lesions. The fourth scan, higher than the fifth scan, offers a view of superior brain structures, including the cerebellum and brainstem. The sixth scan captures the topmost structures, such as the superior sagittal sinus and cortical gyri. These scans are crucial for diagnosing neurological conditions, planning surgeries, and monitoring treatment progress, allowing clinicians to visualize brain anatomy and identify potential issues without invasive procedures.

4.4. **Performance Analysis of Suggested Model.** This section provides a detailed explanation of the performance analysis of the suggested model using varied epochs (ranging from 10 to 50), which represents one complete cycle for presenting the entire training data to the neural network and updating its weights and biases.

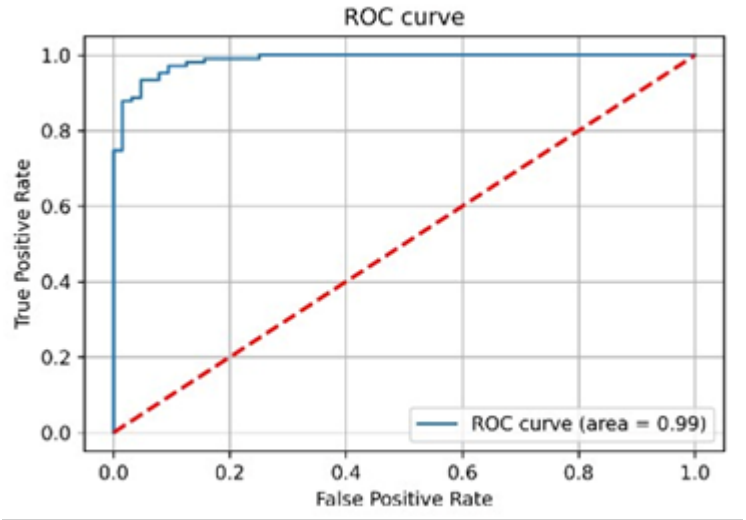

FIGURE 9. ROC curve of suggested model

Figure 9 shows ROC curves representing the performance of the suggested model, with the False Positive Rate (FPR) and True Positive Rate (TPR) ranging from 0 to 100%. This indicates the models and their respective Area Under the Curve (AUC) values. The ROC curves show how well each model distinguishes between classes, with higher AUC

values indicating better classification abilities. The proposed model performs exceptionally well with an AUC of 99%, making it the most effective model based on the AUC value.

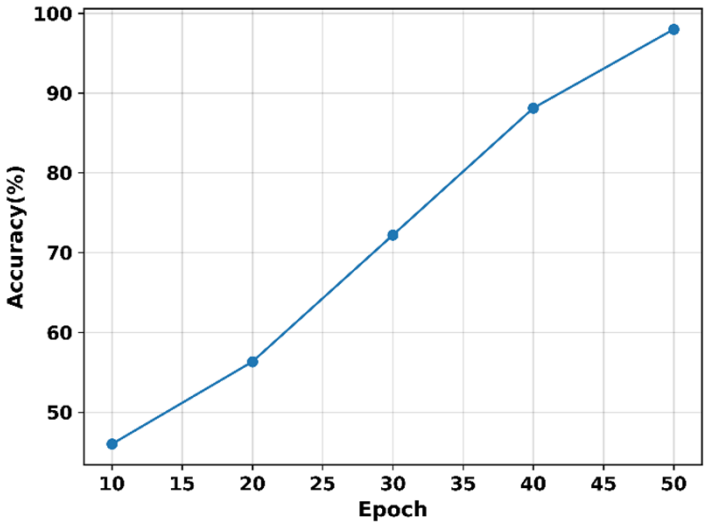

FIGURE 10. Accuracy of suggested model

Figure 10 depicts the accuracy of the suggested model. The process initially begins at the 10 epochs when the accuracy is 44% and it then improves through the process and at 50 epochs, accuracy improves to the peak of 98%. By aggregating predictions from multiple ERTs, ESCCRT reduces overfitting and improves generalization to unseen data, thereby enhancing the overall accuracy of tumor classification and survival prediction.

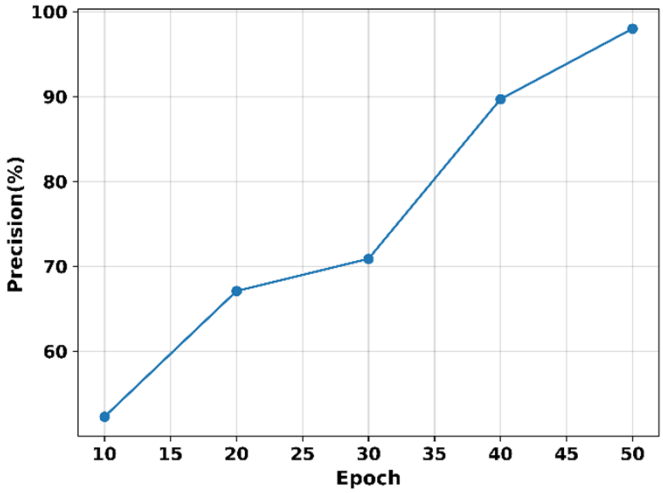

FIGURE 11. Precision of suggested model

Figure 11 depicts the precision of the suggested model. The process initially begins at the 10 epochs when the precision is 52% and it then improves through the process and at 50 epochs, precision improves to the peak of 98%. DMF-SWC operates by analyzing the local structure of the image at multiple scales and identifying vessel-like structures based on their eigenvalues.

This method is particularly sensitive to the precision of vessel detection, ensuring that only true vessel structures are enhanced while minimizing false positives.

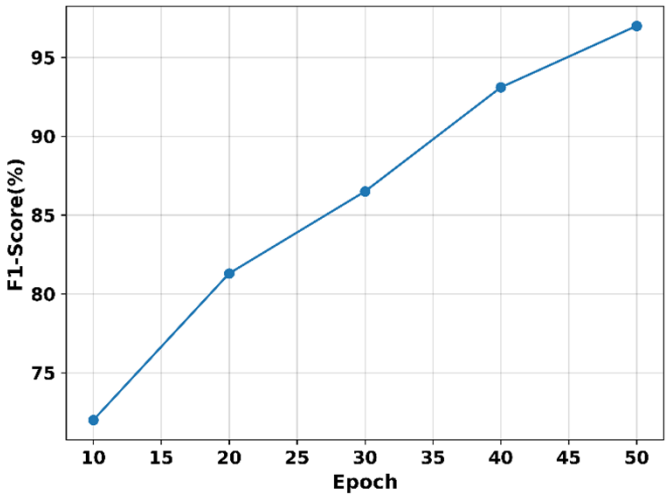

FIGURE 12. F1-Score of suggested model

Figure 12 depicts the F1-Score of the suggested model. The process initially begins at the 10 epochs when the F1-Score is 72% and it then improves through the process and at 50 epochs, F1-Score improves to the peak of 97%. DMF-SWC improves precision by accurately detecting vessel structures and boundaries, reducing false positives. It also enhances recall by minimizing false negatives, ensuring that vessel structures are not missed.

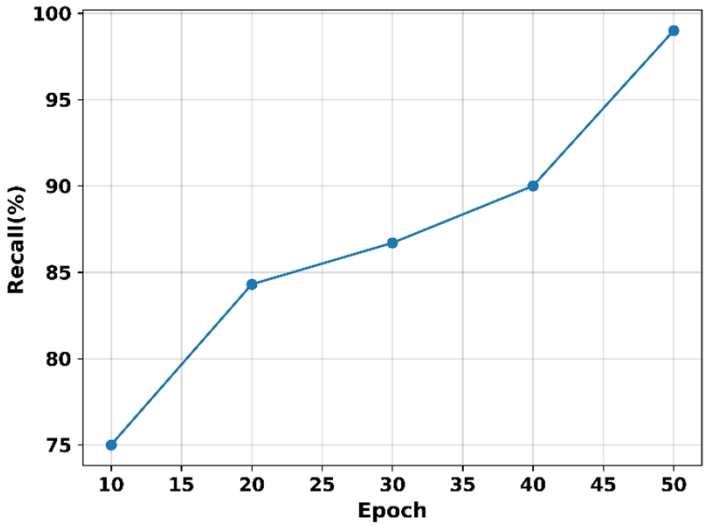

FIGURE 13. Recall of suggested model

Figure 13 depicts the Recall of the suggested model. The process initially begins at the 10 epochs when the Recall is 75% and it then improves through the process and at 50 epochs, Recall improves to the peak of 99%. DMF-SWC enhances recall by effectively detecting and capturing vessel-like structures across multiple scales and contrasts. Its multiscale approach helps in capturing vessels of varying sizes and intensities, thereby minimizing the chances of missing any vessel structure.

Figure 14 depicts the Sensitivity of the suggested model. The process initially begins at the 10 epochs when the Sensitivity is 43% and it then improves through the process and at 50 epochs, Sensitivity improves to the peak of 98%. DMF-SWC enhances sensitivity by

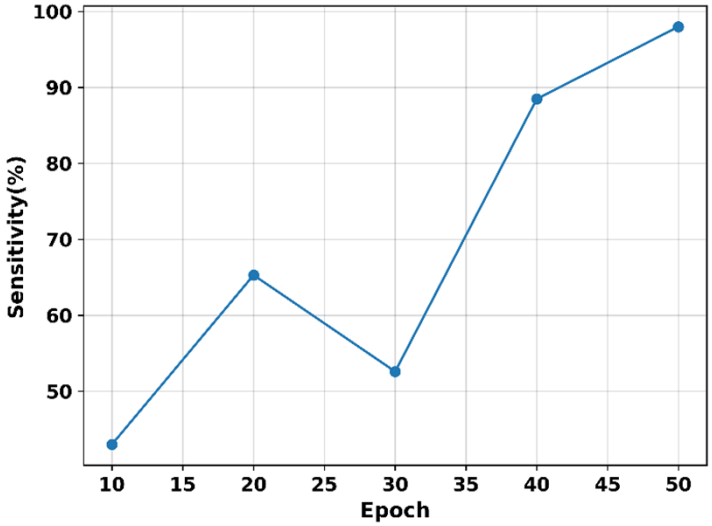

FIGURE 14. Sensitivity of suggested model

effectively detecting and capturing vessel-like structures across multiple scales and contrasts. Its multiscale approach helps in capturing vessels of varying sizes and intensities, therefore reducing the possibility of overlooking any vessel construction.

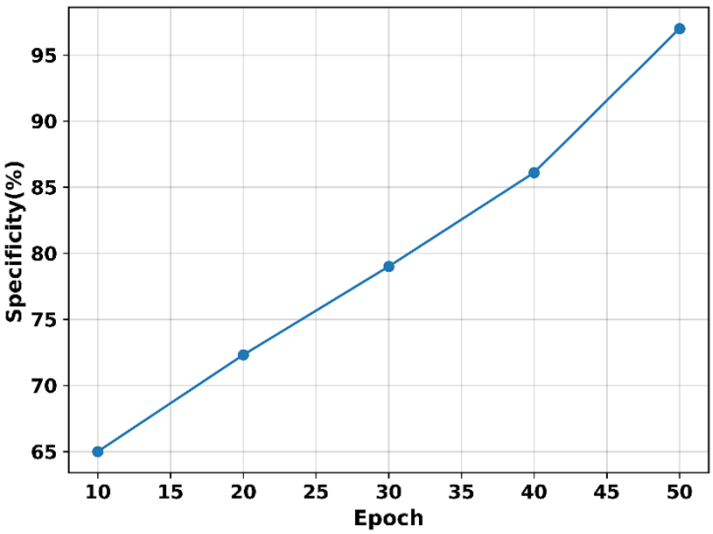

FIGURE 15. Specificity of suggested model

Figure 15 depicts the Specificity of the suggested model. The process initially begins at the 10 epochs when the Specificity is 65% and it then improves through the process and at 50 epochs, Specificity improves to the peak of 98%. ESCCRT improves specificity by efficiently classifying negative instances and minimizing false positives, thereby enhancing the model's ability to distinguish between different classes with higher accuracy.

Figure 16 depicts the Mathews Correlation Coefficient (MCC) of the suggested model. The process initially begins at the 10 epochs when the MCC is 0.65 and it then improves through the process and at 50 epochs, MCC increases to the peak of 0.98. By using ESCCRT, being a decision tree-based classifier, it is known for its ability to handle

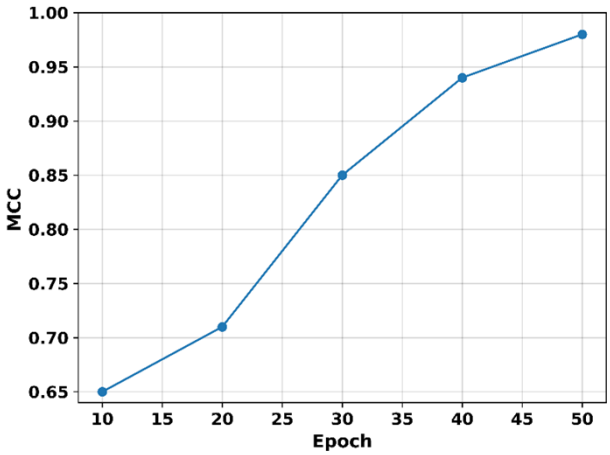

FIGURE 16. MCC of suggested model

complex decision boundaries and hierarchical data structures, that accounts true positives, true negatives, false positives, and false negatives, providing a balanced measure of classification performance which improves MCC.

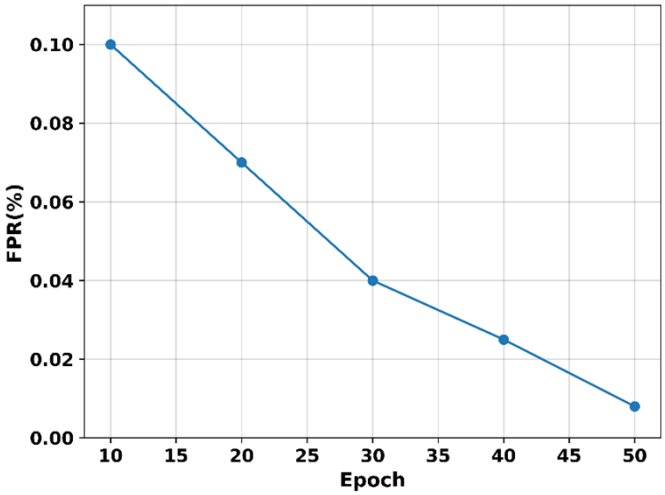

FIGURE 17. FPR of suggested model

Figure 17 depicts the False positive rate (FPR) of the suggested model. The process initially begins at the 10 epochs when the FPR is 0.10% and it then decreases through the process and at 50 epochs, FPR reduces to the rate of 0.008%. FPR measures the ratio of false positives to actual negative instances. ESCCRT, a variant of Random Forests or Decision Trees, improves classification accuracy by reducing false positives and false negatives and its optimization of decision boundaries and ensemble learning techniques helps control FPR by minimizing false positives during classification.

Figure 18 depicts the False Negative Rate (FNR) of the suggested model. The process initially begins at the 10 epochs when the FNR is 4.3% and it then improves through the process and at 50 epochs, FNR decreases to 2.7%. DMF-SWC focuses on enhancing sensitivity and recall, which are metrics directly related to minimizing false negatives by correctly identifying positive instances, which is crucial in medical imaging as it measures the ratio of incorrectly classified negative instances (actual positives) to the total number of actual positive instances to reduce the negative rate of the model.

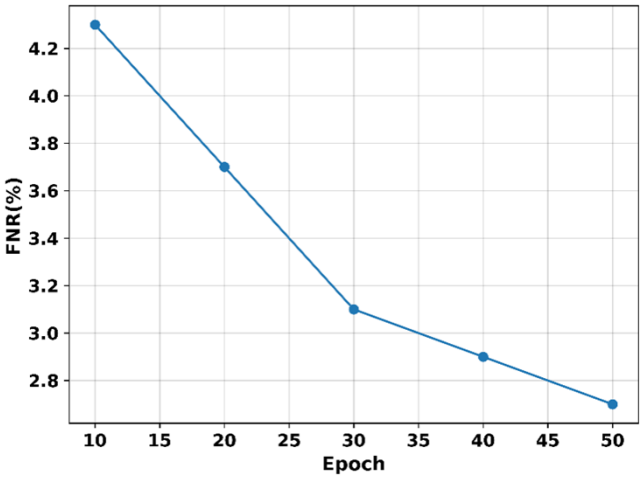

FIGURE 18. FNR of suggested model

4.5. **Comparison of Suggested Model with Other Models.** This section emphasizes the performance of the proposed method by comparing its results with those of existing approaches, using various metrics to showcase the differences.

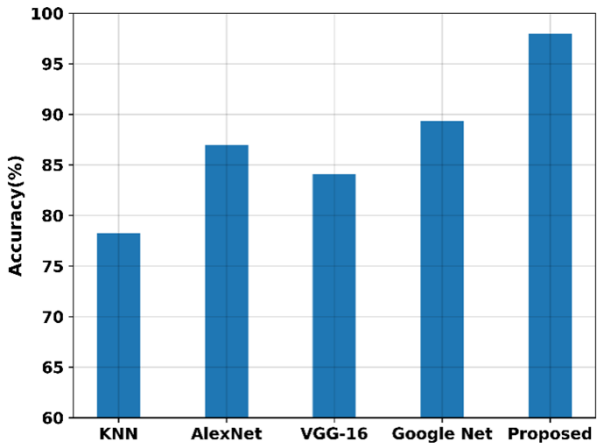

FIGURE 19. Comparison of Suggested Model Accuracy with Other Models

Figure 19 illustrates a comparison of the accuracy of the suggested model with other existing techniques, such as KNN, AlexNet, VGG-16, and GoogleNet. The accuracy of the suggested model obtains the value of 98%, whereas KNN, AlexNet, VGG-16, and GoogleNet are 78%, 87%, 84%, and 89%, respectively. The suggested model achieved high accuracy in brain tumor classification, whereas KNN demonstrated lower accuracy.

Figure 20 illustrates a comparison of the precision of the suggested model with other existing techniques, such as KNN, AlexNet, VGG-16, and GoogleNet. The precision of the suggested model obtains the value of 98% whereas KNN, AlexNet, VGG-16, and GoogleNet are 73%, 94%, 89%, and 96%, respectively. The suggested model exhibited high precision in brain tumor classification, while KNN showed low precision.

Figure 21 illustrates a comparison of the recall of the suggested model with other existing techniques, such as KNN, AlexNet, VGG-16, and GoogleNet. The recall of the suggested model obtains the value of 99% whereas KNN, AlexNet, VGG-16, and GoogleNet are 80%, 95%, 93%, and 95.1%, respectively. The suggested model demonstrated high recall in brain tumor classification, whereas KNN exhibited low recall.

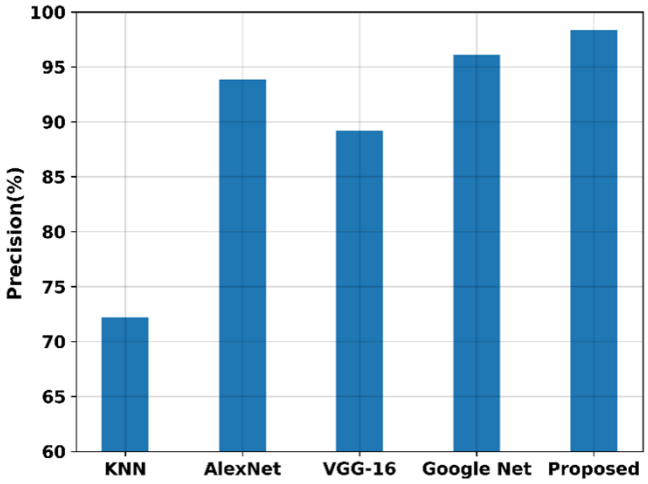

FIGURE 20. Comparison of Suggested Model Precision with Other Models

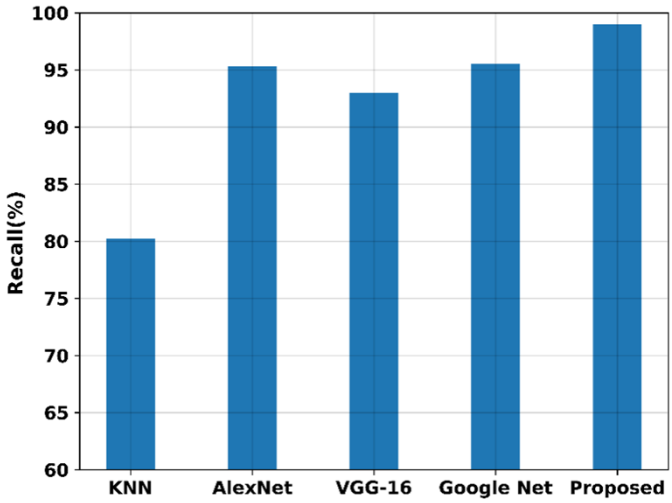

FIGURE 21. Comparison of Suggested Model Recall with Other Models

Figure 22 illustrates a comparison of the F1-score of the suggested model with other existing techniques, such as KNN, AlexNet, VGG-16, and GoogleNet. The F1-score of the suggested model obtains the value of 97% whereas KNN, AlexNet, VGG-16, and GoogleNet are 68%, 88%, 85%, and 90%, respectively. The suggested model achieved a high F1-score in brain tumor classification, whereas KNN obtained a low F1-score.

Figure 23 illustrates a comparison of the Sensitivity of the suggested model with other existing techniques, such as KNN, AlexNet, VGG-16, and GoogleNet. The Sensitivity of the suggested model obtains the value of 98%, whereas KNN, AlexNet, VGG-16, and GoogleNet are 46%, 84%, 81%, and 84%, respectively. The suggested model showed high sensitivity in brain tumor classification, whereas KNN exhibited low sensitivity.

Figure 24 illustrates a comparison of the Specificity of the suggested model with other existing techniques, such as KNN, AlexNet, VGG-16, and GoogleNet. The specificity of the suggested model obtains the value of 98% whereas KNN, AlexNet, VGG-16, and GoogleNet are 50%, 92%, 89%, and 95%, respectively. The specificity of Brain tumor classification of the suggested model was high, whereas the specificity of Brain tumor classification of KNN was low.

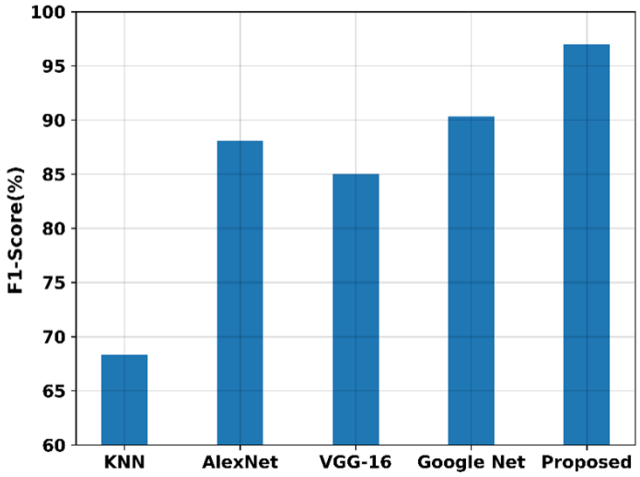

FIGURE 22. Comparison of Suggested Model F1-Score with Other Models

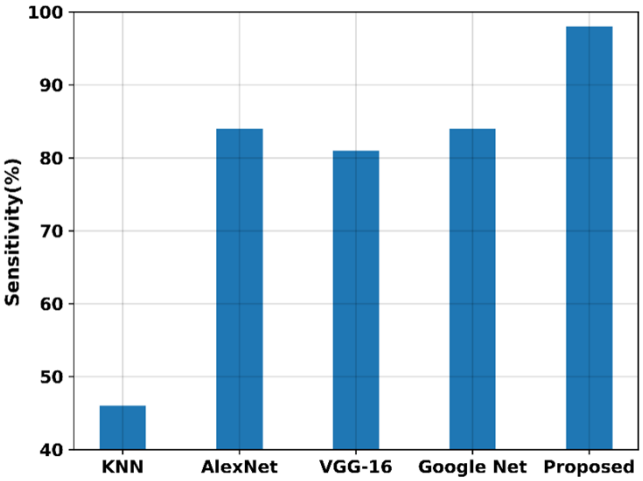

FIGURE 23. Comparison of Suggested Model Sensitivity with Other Models

Figure 25 illustrates a comparison of the FPR of the suggested model with other existing techniques, such as Finetree, Linear discriminant, SVM, and wide neural network. The FPR of the suggested model obtains the value of 0.008% whereas Finetree, Linear discriminant, SVM, and wide neural network are 0.0275%, 0.0125%, 0.10%, and 0.0150%, respectively. The suggested model had a low false positive rate (FPR) in brain tumor classification, while SVM showed a high false positive rate.

Figure 26 illustrates a comparison of the FNR of the suggested model with other existing techniques, such as Finetree, Linear discriminant, SVM, and wide neural network. The FNR of the suggested model obtains the value of 2.7% whereas Finetree, Linear discriminant, SVM, and wide neural network are 7.5%, 4.2%, 5.5%, and 4.6%, respectively. The suggested model had a low false negative rate (FNR) in brain tumor classification, while SVM exhibited a high false negative rate.

Figure 27 presents a comparison of the Matthews correlation coefficient (MCC) between the suggested model and other existing techniques, including ResNet 50, VGG-16, and Inception V3. The MCC of the suggested model achieved a value of 0.98, whereas ResNet 50, VGG-16, and Inception V3 attained MCC values of 0.93, 0.93, and 0.95, respectively.

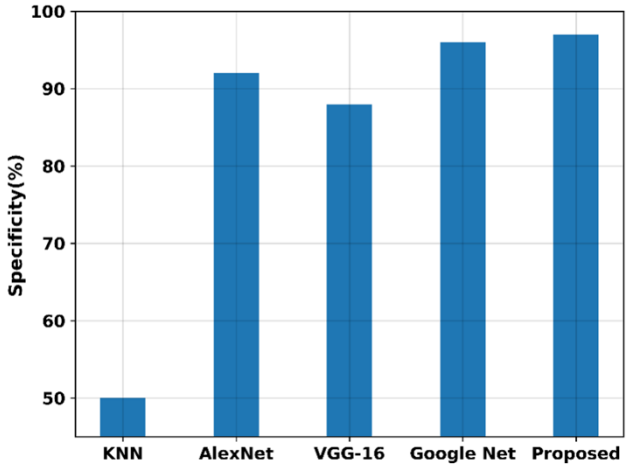

FIGURE 24. Comparison of Suggested Model Specificity with Other Models

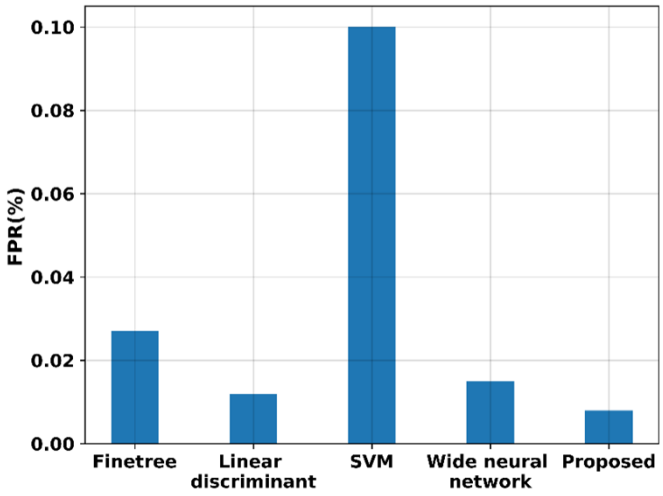

FIGURE 25. Comparison of Suggested Model FPR with Other Models

The MCC for brain tumor classification was high for the suggested model, whereas it was low for ResNet 50 and VGG-16.

Figure 28 illustrates the Receiver Operating Characteristic (ROC) curve to evaluate the performance of various models. It shows multiple ROC curves, each representing the performance of a different model. The graph shows True Positive Rate (TPR) and False Positive Rate (FPR) values, and the models and their respective Area Under the Curve (AUC) values. The proposed model has an AUC of 99%, outperforming InceptionV3, VGG16, ResNet50, and Random Classifier. Higher AUC values indicate better model performance in correctly classifying positive and negative instances. The proposed model, with an AUC of 99%, is the most effective based on the AUC value. Overall, the graph provides valuable insights into the classification abilities of different models.

Overall, the Multiscale Frangi susceptibility Cat Randomized Gaussian Gray-level Matrix outperforms other existing methods in brain tumor classification. It achieves high accuracy, precision, recall, F1-score, sensitivity, specificity, FPR, FNR, and MCC against other prominent techniques like KNN, AlexNet, VGG-16, GoogleNet, SVM, and more. The suggested model consistently achieves superior results across all metrics, demonstrating high accuracy of 98%, precision of 98%, recall of 99%, F1-score of 97%, sensitivity

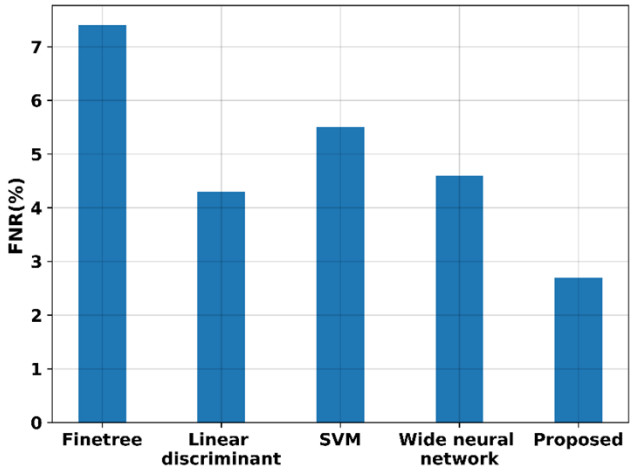

FIGURE 26. Comparison of Suggested Model FNR with Other Models

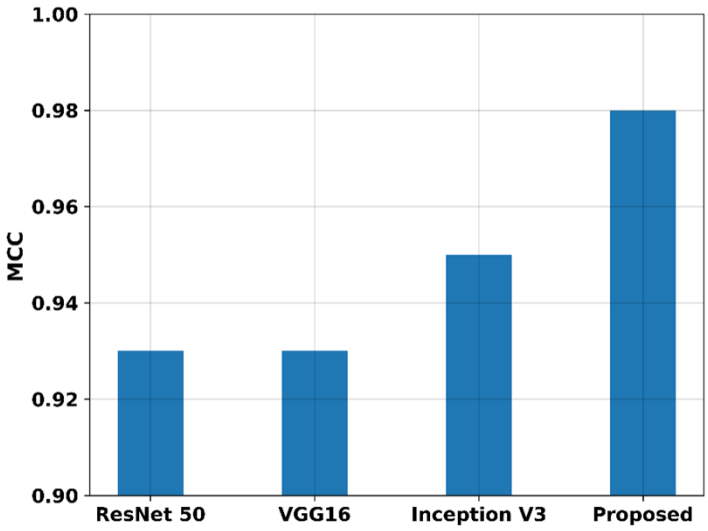

FIGURE 27. Comparison of Suggested Model MCC with Other Models

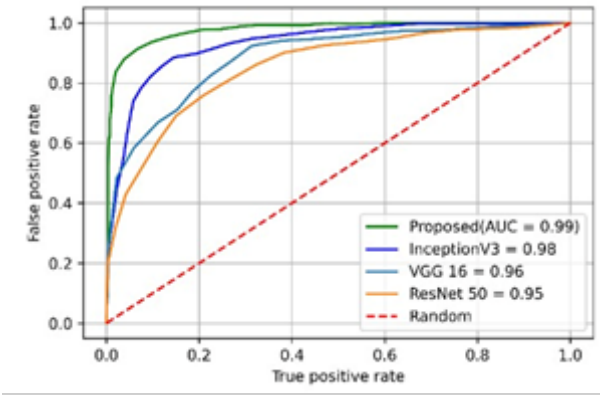

FIGURE 28. Comparison of Proposed Model ROC-AUC Curve with Other Models

of 98%, specificity of 98%, low FPR of 0.008%, low FNR of 2.7%, and a high MCC of

0.98. These findings underscore its effectiveness in brain tumor classification compared to traditional and deep learning models, as illustrated in the ROC-AUC curve, where it outperforms competitors with an AUC of 99%.

5. **Conclusion.** Recognizing brain tumor is crucial as they lead to a range of neurological disorders. For identifying brain tumor classification and to predict the survival rate, an innovative methodology was proposed, namely Multiscale Frangi susceptibility Cat Randomized Gaussian Gray-level Matrix. This framework, integrating Dynamic Multiscale Frangi Susceptibility-Weighted Contrast (DMF-SWC), Extreme Spatial Channel Cat Randomized Trees (ESCCRT), and Gaussian Gray-level size length matrix represents a significant advancement in brain tumor classification using MRI scans. This model addresses critical challenges in accurate tumor characterization by leveraging advanced imaging techniques and machine learning algorithms. DMF-SWC enhances the visualization of cerebral venous structures and improves precision of 98%, recall of 99%, F1-score of 97%, sensitivity of 98% and FNR at 2.7% in detecting vessel-like patterns across varying scales and contrasts. This capability is crucial for distinguishing subtle vascular anomalies crucial for accurate tumor delineation. Meanwhile, ESCCRT, incorporating Spatial Channel-Wise Attention and Extreme Randomized Trees within a stacked CNN architecture, effectively integrates features related to venous collateralization patterns and peritumoral edema characteristics. This integration not only enhances accuracy of 98%, specificity of 98%, MCC of 0.98, low FPR of 0.008%, while also enhancing the model's capability to accurately classify various types of brain tumors. Furthermore, achieving an AUC of 99% in ROC analysis confirms the model's exceptional capability in distinguishing between tumor and non-tumor instances, highlighting its superiority over existing methods and then, GGSLM classifies survival rate prediction accurately. Overall, this novel approach not only advances the state-of-the-art in brain tumor classification but also promises significant improvements in patient care by providing more accurate diagnostic and prognostic information.

REFERENCES

[1] T. Rahman, and M.S. Islam, "MRI brain tumor detection and classification using parallel deep convolutional neural networks," *Measurement: Sensors,* vol. 26, 2023, pp. 100694.

[2] A.A. Asiri, A. Shaf, T. Ali, M. Aamir, M. Irfan, S. Alqahtani, K.M. Mehdar, H.T. Halawani, A.H. Alghamdi, A.F.A. Alshamrani, and S.M. Alqhtani, "Brain tumor detection and classification using fine-tuned CNN with ResNet50 and U-Net model: A study on TCGA-LGG and TCIA dataset for MRI applications," *Life,* vol. 13, no. 7, 2023, pp. 1449.

[3] M. Uvaneshwari, and M. Baskar, "Computer-Aided Diagnosis Model Using Machine Learning for Brain Tumor Detection and Classification," *Comput. Syst. Sci. Eng.,* vol. 46, no. 2, 2023, pp. 1811-1826.

[4] S. Saeedi, S. Rezayi, H. Keshavarz, and R. Niakan S. Kalhori, "MRI-based brain tumor detection using convolutional deep learning methods and chosen machine learning techniques," *BMC Medical Informatics and Decision Making,* vol. 23, no. 1, 2023, pp. 16.

[5] D.N. Louis, A. Perry, P. Wesseling, D.J. Brat, I.A. Cree, D. Figarella-Branger, C. Hawkins, H.K. Ng, S.M. Pfister, G. Reifenberger, and R. Soffietti, "The 2021 WHO classification of tumors of the central nervous system: a summary," *Neuro-oncology,* vol. 23, no. 8, 2021, pp. 1231-1251.

[6] B. Jena, S. Saxena, G.K. Nayak, A. Balestrieri, N. Gupta, N.N. Khanna, J.R. Laird, M.K. Kalra, M.M. Fouda, L. Saba, and J.S. Suri, "Brain tumor characterization using radiogenomics in artificial intelligence framework," *Cancers,* vol. 14, no. 16, 2022, pp. 4052.

[7] S.M. Alzahrani, and A.M. Qahtani, "Knowledge distillation in transformers with tripartite attention: Multiclass brain tumor detection in highly augmented MRIs," *Journal of King Saud University-Computer and Information Sciences,* vol. 36, no. 1, 2024, pp. 101907.

[8] P. Priyadarshini, P. Kanungo, and T. Kar, "Multigrade Brain tumor classification in MRI images using Fine-tuned EfficientNet," *e-Prime-Advances in Electrical Engineering, Electronics and Energy,* 2024, p. 100498.

[9] J. Amin, M. Sharif, M. Yasmin, and S.L. Fernandes, "A distinctive approach in brain tumor detection and classification using MRI," *Pattern Recognition Letters,* vol. 139, 2020, pp. 118-127.

[10] M.A. Hamid, and N.A. Khan, "Investigation and classification of MRI brain tumors using feature extraction technique," *Journal of Medical and Biological Engineering,* vol. 40, 2020, pp. 307-317.

[11] M.S.I. Khan, A. Rahman, T. Debnath, M.R. Karim, M.K. Nasir, S.S. Band, A. Mosavi, and I. Dehzangi, "Accurate brain tumor detection using deep convolutional neural network," *Computational and Structural Biotechnology Journal,* vol. 20, 2022, pp. 4733-4745.

[12] B. Kokila, M.S. Devadharshini, A. Anitha, and S.A. Sankar, "Brain tumor detection and classification using deep learning techniques based on MRI images," *Journal of Physics: Conference Series,* vol. 1916, no. 1, 2021, pp. 012226.

[13] C. Srinivas, N.P. KS, M. Zakariah, Y.A. Alothaibi, K. Shaukat, B. Partibane, and H. Awal, "Deep transfer learning approaches in performance analysis of brain tumor classification using MRI images," *Journal of Healthcare Engineering,* 2022, pp. 1-12.

[14] A. Zadeh Shirazi, E. Fornaciari, N.S. Bagherian, L.M. Ebert, B. Koszyca, and G.A. Gomez, "DeepSurvNet: deep survival convolutional network for brain cancer survival rate classification based on histopathological images," *Medical & Biological Engineering & Computing,* vol. 58, 2020, pp. 1031-1045.

[15] D. Lamrani, B. Cherradi, O. El Gannour, M.A. Bouqentar, and L. Bahatti, "Brain tumor detection using MRI images and convolutional neural network," *International Journal of Advanced Computer Science and Applications,* vol. 13, no. 7, 2022.

[16] Z. Jia, and D. Chen, "Brain tumor identification and classification of MRI images using deep learning techniques," *IEEE Access,* 2020.

[17] Y. Bhanothu, A. Kamalakannan, and G. Rajamanickam, "Detection and classification of brain tumor in MRI images using deep convolutional network," *2020 6th International Conference on Advanced Computing and Communication Systems (ICACCS),* 2020, pp. 248-252.

[18] M.M. Badža, and M.Č. Barjaktarović, "Classification of brain tumors from MRI images using a convolutional neural network," *Applied Sciences,* vol. 10, no. 6, 2020, pp. 1999.

[19] C.H. Toh, and M. Castillo, "Peritumoral brain edema volume in meningioma correlates with tumor fractional anisotropy but not apparent diffusion coefficient or cerebral blood volume," *Neuroradiology,* vol. 63, 2021, pp. 1263-1270.

[20] M. Islam, V.S. Vibashan, V.J.M. Jose, N. Wijethilake, U. Utkarsh, and H. Ren, "Brain tumor segmentation and survival prediction using 3D attention UNet," *BrainLes 2019,* Springer, 2020, pp. 262-272.

[21] L. Curtin, P. Whitmire, H. White, M.M. Mrugala, L.S. Hu, and K.R. Swanson, "Morphological Metrics of Magnetic Resonance Imaging of Glioblastoma as Biomarkers of Prognosis," *bioRxiv,* 2021.

[22] H. Kibriya, R. Amin, J. Kim, M. Nawaz, and R. Gantassi, "A novel approach for brain tumor classification using an ensemble of deep and hand-crafted features," *Sensors,* vol. 23, no. 10, 2023, pp. 4693.

[23] A. Sarkar, M. Maniruzzaman, M.A. Alahe, and M. Ahmad, "An effective and novel approach for brain tumor classification using AlexNet CNN feature extractor and multiple eminent machine learning classifiers in MRIs," *Journal of Sensors,* 2023.

[24] K.V. Archana, and G. Komarasamy, "A novel deep learning-based brain tumor detection using the Bagging ensemble with K-nearest neighbor," *Journal of Intelligent Systems,* vol. 32, no. 1, 2023.

[25] E. Ghafourian, F. Samadifam, H. Fadavian, P. Jerfi Canatalay, A. Tajally, and S. Channumsin, "An ensemble model for the diagnosis of brain tumors through MRIs," *Diagnostics,* vol. 13, no. 3, 2023, pp. 561.

[26] D. Zhong, J. Wang, Y. Guo, Y. Liu, J. Chen, and T. Xu, "A Frangi filter aided deep learning approach for palaeochannel recognition," *Geophysical Journal International,* vol. 236, no. 3, 2024, pp. 1526-1544.

[27] B. Li, H. Ren, X. Jiang, F. Miao, F. Feng, and L. Jin, "SCEP—A new image dimensional emotion recognition model based on spatial and channel-wise attention mechanisms," *IEEE Access,* vol. 9, 2021, pp. 25278-25290.

[28] N. Nguyen, T. Duong, T. Chau, V.H. Nguyen, T. Trinh, D. Tran, and T. Ho, "A proposed model for card fraud detection based on Catboost and deep neural network," *IEEE Access,* vol. 10, 2022, pp. 96852-96861.

[29] F. Li, H. Gong, B. Chen, C. Zhou, and L. Guo, "Analysis of the contribution rate of the influencing factors to land subsidence in the Eastern Beijing plain, China based on extremely randomized trees (ERT) method," *Remote Sensing,* vol. 12, no. 18, 2020, pp. 2963.

[30] I. Abd El Kader, G. Xu, Z. Shuai, S. Saminu, I. Javaid, and I. Salim Ahmad, "Differential deep convolutional neural network model for brain tumor classification," *Brain Sciences,* vol. 11, no. 3, 2021, pp. 352.

[31] U. Zahid, I. Ashraf, M.A. Khan, M. Alhaisoni, K.M. Yahya, H.S. Hussein, and H. Alshazly, "Brain-Net: optimal deep learning feature fusion for brain tumor classification," *Computational Intelligence and Neuroscience,* vol. 2022, 2022, pp. 1465173.

[32] A.U. Haq, J.P. Li, R. Kumar, Z. Ali, I. Khan, M.I. Uddin, and B.L.Y. Agbley, "MCNN: a multi-level CNN model for the classification of brain tumors in IoT-healthcare system," *Journal of Ambient Intelligence and Humanized Computing,* vol. 14, no. 5, 2023, pp. 4695-4706.